

INDIANA & MICHIGAN ELECTRIC COMPANY

P.O. BOX 16631
COLUMBUS, OHIO 43216

January 9, 1987
AEP:NRC:0514R

Donald C. Cook Nuclear Plant Unit Nos. 1 and 2
Docket Nos. 50-315 and 50-316
License Nos. DPR-58 and DPR-74
AUXILIARY BUILDING CRANE TRAVEL
LOAD BLOCK DROP ANALYSIS

Mr. Harold R. Denton, Director
Office of Nuclear Reactor Regulation
U.S. Nuclear Regulatory Commission
Washington, D.C. 20555

- References:
- 1) Our Letter AEP:NRC:05140, dated February 14, 1986
 - 2) NRC Safety Evaluation Report (SER) dated February 27, 1986
 - 3) NUREG-0612, "Control of Heavy Loads in Nuclear Power Plants," dated July 1980

Dear Mr. Denton:

This letter and its attachments transmit a load drop analysis of the main load block of the auxiliary building crane of the Donald C. Cook Nuclear Plant. As noted in Reference 1 and the NRC Safety Evaluation Report (Reference 2), we were required to complete a load drop analysis for the main load block within one year of the date of that SER. Attachment 1 contains the load drop analysis that was performed for us by Exxon Nuclear Company (ENC), the suppliers of our current spent fuel pool racks. Attachment 2 is an independent evaluation of the mechanical analysis portions of the ENC report noted above by our consultant Dr. J. D. Stevenson of Stevenson & Associates (S&A). The criticality and radiological consequences sections of Attachment 1 have been reviewed by AEP personnel.

The attached analysis concludes that in the unlikely event the load block should fall from its maximum height, it will strike the top of the spent fuel pool racks. For the postulated accident, the load block itself will be unable to penetrate the upper grid portion of the racks and the kinetic energy of the block will be absorbed by crushing the upper structure of the fuel rack. However, the hook may cause of the rupture of the grid, with a subsequent penetration of the hook to a maximum depth of 29.5" into the active fuel region. If such penetration should occur, a maximum of four fuel assemblies could be damaged.

REC'D W/CHECK
325-0367

A033
1/11

8701200057 870109
PDR ADCK 05000315
P PDR



Vertical column of faint, illegible characters on the left side of the page.

Horizontal line of faint, illegible characters in the middle of the page.

Small cluster of faint, illegible characters.

Horizontal line of faint, illegible characters near the bottom of the page.

The radiological consequences and the potential for criticality as a result of this accident have been examined. It was conservatively assumed that this will result in four times the release cited in the Updated FSAR for the consequences of a fuel-handling accident in the auxiliary building. In this case, the potential two-hour doses that a person would receive at the site boundary could be as high as 7.2 rem to the thyroid and 2.12 rem whole body. Although this is well below the 10 CFR 100 limits and the restrictions cited in Reference 3 (i.e., one quarter of the 10 CFR 100 limits), it requires that radioactive iodine be filtered through the spent fuel pool filter system.

A criticality analysis was performed assuming that the four damaged fuel assemblies were moved to their most reactive configuration. Analysis of this configuration was performed using a 2 x 2 array of damaged fuel assemblies at the center of each of an infinite number of arrays of 10 x 10 undamaged fuel assemblies of infinite length. The result of this calculation was a Keff of 0.94, at a one-sided 95% confidence level based on use of the KENO V computer code. This is below the value of Keff of 0.95, which is suggested as an acceptable limit by Section 2.2 of Reference 3.

Based on the above, we believe that even though the actual weight of the load block is approximately 4.25 tons, it should not be considered a heavy load for the purpose of compliance with Technical Specification (T/S) 3.9.7, provided the spent fuel pool ventilation is operable and the auxiliary building is under the negative pressure required by T/S 3.9.12. In the event the above conditions of T/S 3.9.12 cannot be complied with, we will administratively require the main hoist to be deenergized and carry no load on the main hook when the load block is moved over the pool. This latter condition is the same as the current requirement of T/S 3.9.7. We believe that an analysis of the handling of heavy loads can take credit for the charcoal filters, as noted in Appendix A, Item 1 (4) of Reference 3, provided that we meet the conditions of T/S 3.9.12 with respect to auxiliary building negative pressure.

A response is requested from the NRC staff by February 28, 1987, in order to ensure continued operation of the Donald C. Cook Nuclear Plant. The reason for this is that a footnote has been added to T/S 3.9.7 that expires on that date. The purpose of that footnote, as stated in Reference 2, was to allow sufficient time to complete an analysis of the consequences of a postulated drop of the main load block. We believe that this letter and its attachments fulfill that requirement.

A check in the amount of \$150.00 has been enclosed for NRC processing of this submittal.

This document has been prepared following Corporate procedures which incorporate a reasonable set of controls to insure its accuracy and completeness prior to signature by the undersigned.

Very truly yours,



M. P. Alexich
Vice President

EBK
1/9/87

cm

Attachments

cc: John E. Dolan
W. G. Smith, Jr. - Bridgman
R. C. Callen
G. Bruchmann
G. Charnoff
NRC Resident Inspector - Bridgman
J. G. Keppler - Region III

ATTACHMENT 1 TO AEP:NRC:0514R

JAN 08 1987

EXXON NUCLEAR COMPANY, INC.2101 HORN RAPIDS ROAD, PO BOX 130, RICHLAND, WA 99352
509-375 8100 TELEX 15-2878January 6, 1986
AJM-87-001

*Rbb
1/8/87*

Mr. R. B. Bennett
American Electric Power
1 Riverside Plaza
P. O. Box 16631
Columbus, Ohio 43216-6631

Dear Mr. Bennett:

Subject: D. C. Cook Spent Fuel Pit Load Drop Analysis

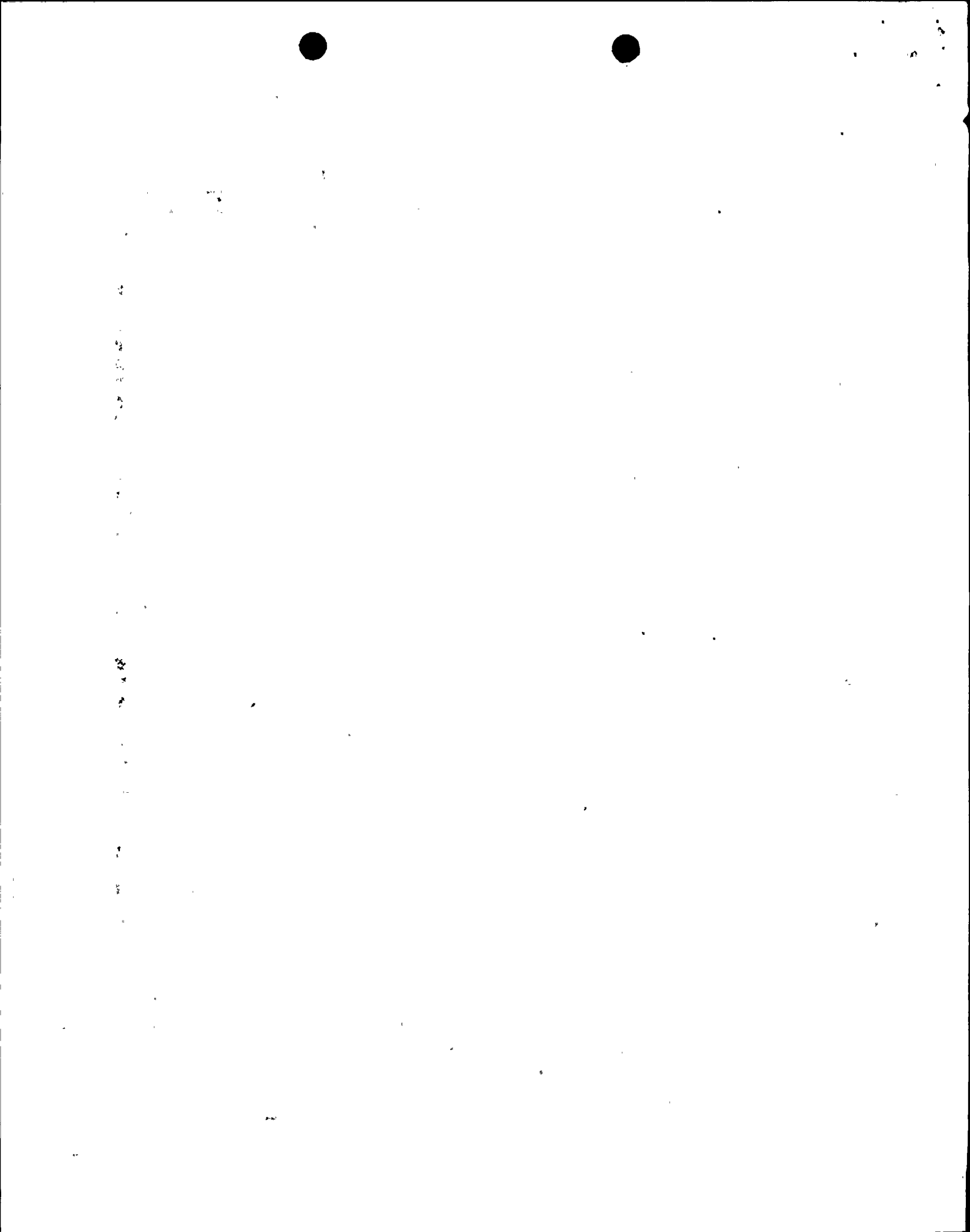
This is in response to your request for ENC to perform an analysis of the consequences of dropping the 4.25 ton hook/block assembly into the spent fuel pit from its full height.

It was concluded from the analysis that the accident will not cause a criticality incident, and that the released radiation dose as a result of such an accident is less than one-fourth of the 10 CFR 100 limits, i.e., 75 rem thyroid and 6.25 whole body. Furthermore, the kinetic energy limit of 240,000 in-lbs recommended in NUREG-612 can be applicable to the Cook Plant.

The analysis is included as three appendices to this report. Appendix A is the mechanical analysis which predicts the extent of the damage, Appendix B shows the results of a confirmatory test, and Appendix C shows the inputs to the criticality analysis.

Mechanical Analysis

The sketch on page A-1 illustrates the geometry of the problem. It is assumed that the hook/block is dropped from a height of 39 feet above the surface of the pool. It then travels an additional distance of 23.7 feet through the water before impacting the top of the fuel rack. The velocity at the time of impact with the water surface is 50.1 ft/sec. Due to the drag and buoyancy of the water, the velocity of the hook/block increases only slightly as it drops through the water so that the velocity of impact with the top surface of the fuel storage rack is 51.6 ft/sec. This is shown on page A-5. The grid of bars near the top of the rack, together with the upper portions of the fuel storage cells, will absorb the impacting energy of the hook/block. The sketch on page A-17 shows the position of the hook/block relative to one of the fuel storage cells when it finally comes to rest. It can be seen that the hook will penetrate to a point 29.5 inches into the active fuel region. The block itself will not penetrate the grid, but will crush the top 19 inches of fifteen fuel storage cells. The sketch on page A-1 shows a top view. The hook will damage approximately four assemblies seriously, and will cause superficial damage to several surrounding assemblies.



It is estimated on page A-18 that 360 kgs of uranium will be released in the form of pellets and fragments which will fall through the water. Most of this debris will be trapped at the top of the first undamaged fuel assembly spacer. The radiation dose total release will be 7.2 rem thyroid and 2.12 rem whole body, as calculated on page A-18.

These mechanical calculations are based on the principle that the hook/block will continue to move through the structure until the kinetic energy, which was available upon impact, is dissipated by gross distortion and crushing of the upper structure of the fuel storage rack. The lower portions of the rack and the fuel assemblies will experience some vibration, but this will be restrained by the spacers and well damped by the water. Furthermore, the length of time required to bring the hook/block to a stop from the time of impact with the fuel rack is only 124 msec. Since the fuel assembly will have a lateral period of vibration of 500 to 1000 msec, the energy will have been absorbed before the lower sections of the fuel assemblies receive any lateral dynamic forces. The longitudinal resonant frequencies are higher, but only the elastic components of the longitudinal waves will be transmitted any appreciable distance. These elastic waves will not produce any significant damage.

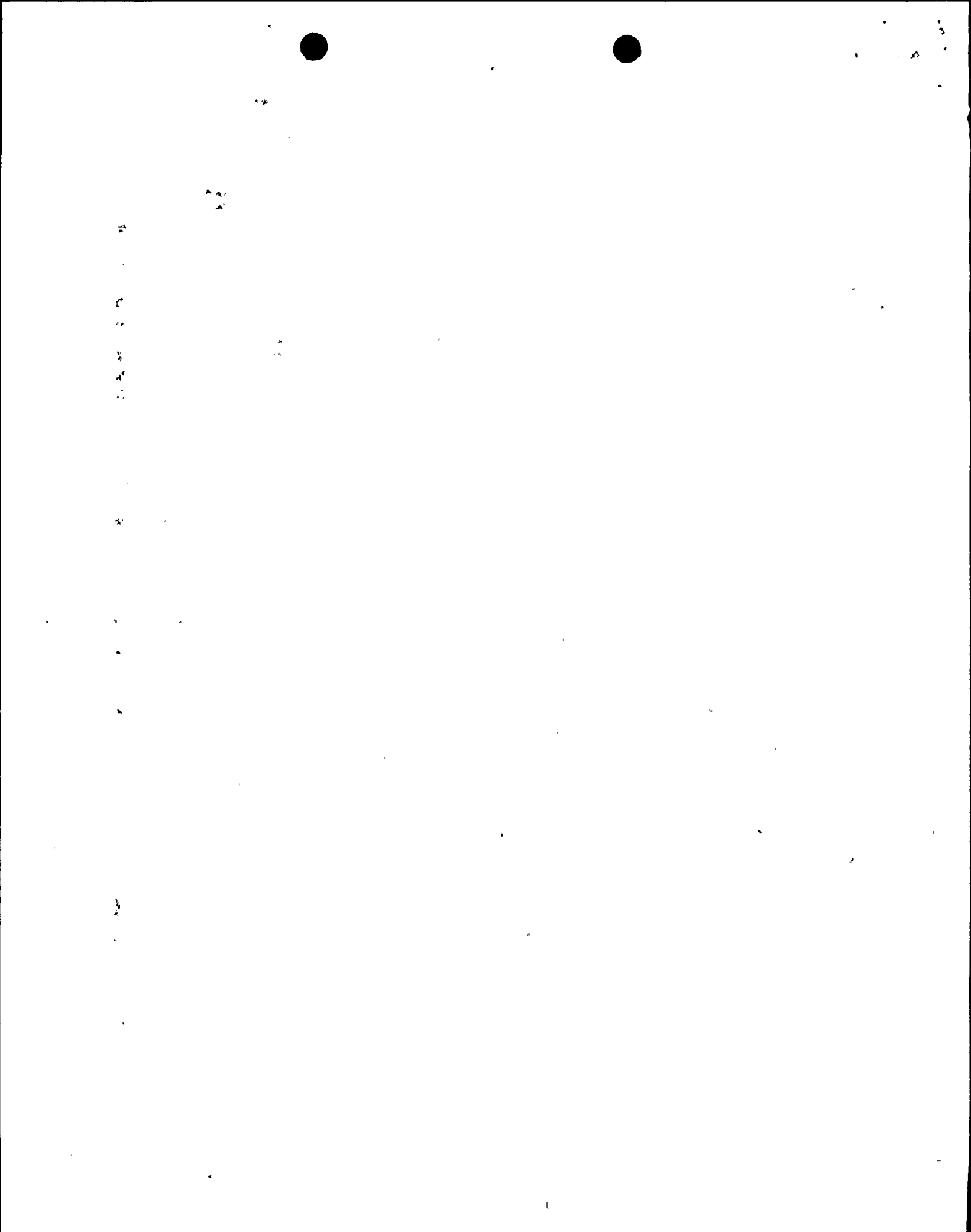
Criticality Analysis

The maximum credible reactivity condition was conservatively modeled.

An infinite array of infinite length rack modules (10x10 bundle array per module) was modeled. Each module contained 96 undamaged bundles and four damaged bundles. The four damaged bundles were conservatively assumed to be in a 2x2 array in the center of the module.

The nominal dimensions of the storage racks were used in all cases. Nominal new fuel dimensions were used for the pellet and clad. All pellets were 95% Theoretical Density UO₂ with an enrichment of 4.0%. The undamaged bundles were modeled at the nominal rod pitch (0.496"), while the damaged bundles were modeled with the 0.5272" rod pitch. Thus, the damaged bundle was expanded to fill the entire storage cell. This is the most reactive configuration in that the bundle moderation has been improved, the bundle size has been increased, and the water gap between the damaged bundle and its absorber plate has been decreased. The absorber plate was modeled as B₄C with a B-10 loading of 0.020 gm per square cm. This is considerably lower than the minimum certified value of 0.0234 gm per square cm, and is therefore, conservative. (See reference 6).

The system described was explicitly modeled using KENO-Va and 16 group cross sections with resonance self-shielding corrections by BONAMI. Replicate calculations using the 27 group ENDF/B-IV cross section library prepared by NITAWL were also performed. All codes and cross sections are part of the SCALE (reference 5) system which has been extensively benchmarked against data from critical experiments. A listing of the KENO input is provided for details on the model. A listing of the input to NITAWL is also provided for details of cross section preparation.



The KENO k-eff for this worst case model is 0.934 +/- 0.0045 using 16 group cross sections, and 0.935 +/- 0.0040 using 27 group cross sections. Therefore, there is no evidence of differences due to cross section sets.

Supplementary benchmarking of the methods employed were performed using data from reference 7. All of the cases selected employed absorber plates between bundles; i.e., they are close to the conditions of this analysis. The average and standard deviation of the calculational biases for the nine cases analyzed (16 group) were 0.0021 and 0.0019, respectively. Pooling the variances from KENO and the bias determination results in an overall standard deviation of 0.0049. The k-eff from KENO was calculated using 103 generations of 400 neutrons. The one-sided 95% probability Student t with 100 degrees of freedom is 1.66.

The corresponding one-sided 95% confidence upper limit on the k-eff is:

$$k\text{-eff (95\% UL)} = 0.934 - 0.0021 + 1.66 * 0.0049 = 0.940$$

Therefore, the k-eff is less than the limit of 0.95 with 95% confidence.

Very truly yours,

AJ Martenson
A. J. Martenson
Mechanical Design Consultant

LD Gerrald
L. D. Gerrald
Criticality Safety Specialist

AJM:sh
Attachments

Mechanical Analysis Review & Approval: RG Hill 1/7/87
R. G. Hill
Senior Engineer
Date

Criticality Analysis Review & Approval: J. E. Pieper 1/7/87
J. E. Pieper
Corporate Licensing-
Quality Assurance Reviewer
(Criticality)
Date

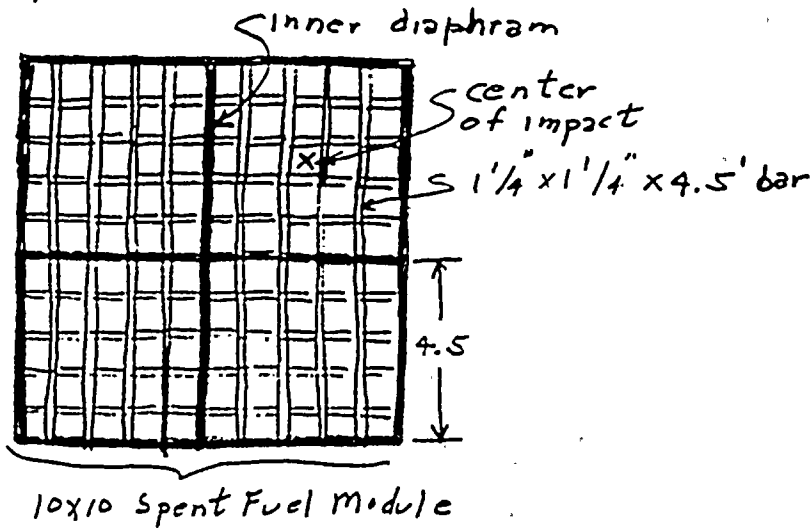
Fuel Design Approval: G. J. Busselman 1/8/87
G. J. Busselman, Manager
Fuel Design
Date

- xc: CA Brown
GJ Busselman
LD Gerrald (2)
RG Hill
AJ Martenson (2)
JE Pieper
RB Stout

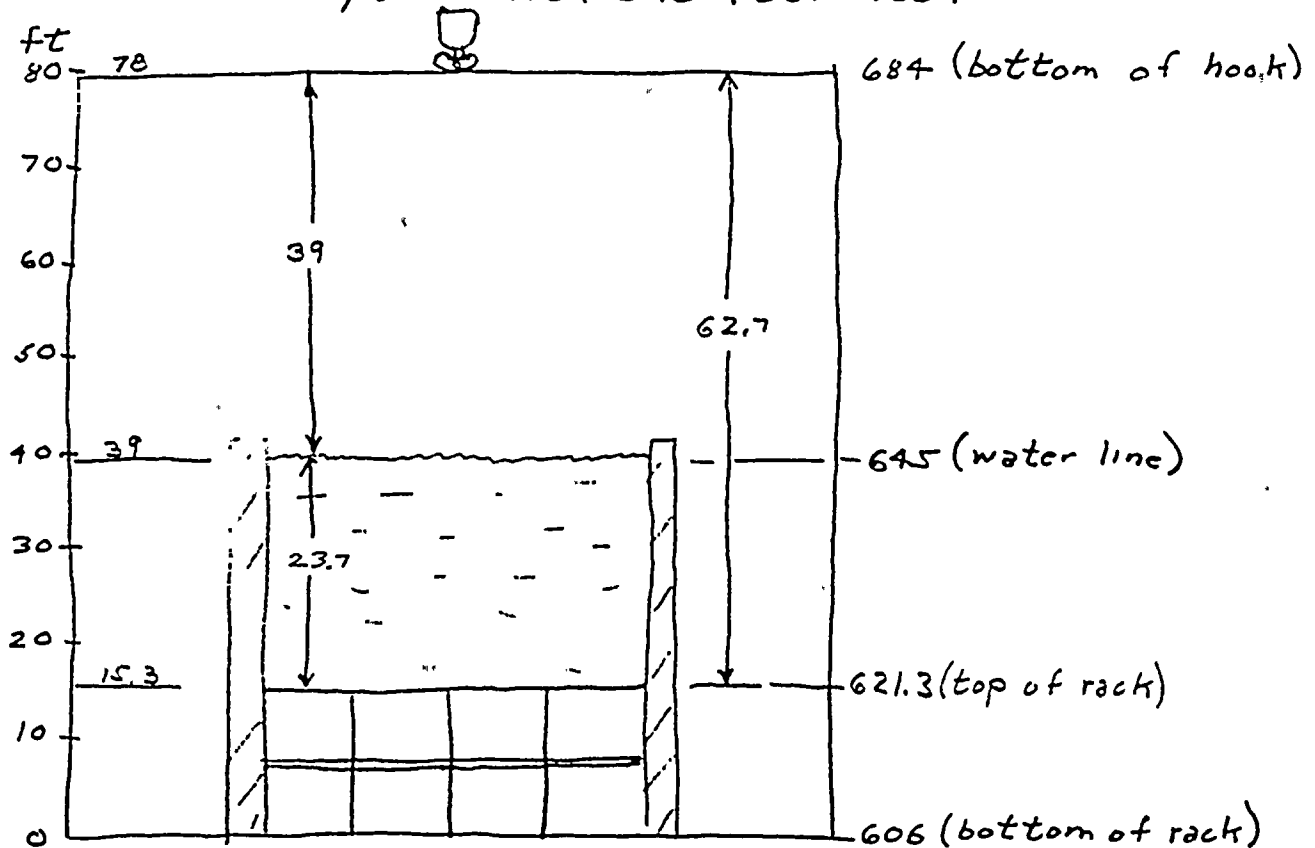
REFERENCES

1. Handbook of Hydraulic Resistance, Coefficients of Local Resistance and of Friction, I.E. Idel'chik , AEC-tr-6630, Published for the U.S. Atomic Energy Commission and the National Science Foundation, Washington, D.C. by the Israel Program for Scientific Translations, 1960, Available from the U.S. Department of Commerce-Clearinghouse for Federal Scientific and Technical Information, Springfield, Va. 22151.
2. Formulas for Stress and Strain, Raymond J. Roark, Third Edition, McGraw Hill Book Company, Inc., 1954.
3. Source Book on Stainless Steels, Compiled by The Periodical Publication Department of the American Society for Metals, Copyright 1976.
4. Stainless Steel Cold-Formed Structural Design Manual, 1974 Edition, American Iron and Steel Institute, 1000 16th Street, NW, Washington, D.C. 20036.
5. "SCALE: A Modular Code System for Performing Standardized Computer Analyses for Licensing Evaluation", NUREG/CR-0200.
6. "DC Cook Units 1 & 2, New and Spent Fuel Storage Array Criticality Safety Analyses", XN-NF-81-47(P), Rev. 2.
7. Baldwin, M.N., et al, "Critical Experiments Supporting Close Proximity Water Storage of Power Reactor Fuel", BAW-1484-7.

Assume that the hook/block impacts the center of one quadrant of one of the 10x10 spent fuel modules. This would do the maximum damage since the inner diaphragms would not participate in the energy absorption. Drawing XN-NS-D-056 shows the upper grid structure for a 10x10 spent fuel module.



Determine the energy of the hook/block at the time of impact with the fuel rack



Velocity of impact with water = $V_0 = \sqrt{2gh}$
 $= \sqrt{2 \times 32.2 \frac{ft}{sec^2} \times 39 ft} = 50.1 ft/sec$

Calc the drag force in the water

Viscosity of water = $\nu = .712 \times 10^{-5} ft^2/sec$

Reynold's number = $\frac{V_0 D}{\nu} = \frac{50.1 \frac{ft}{sec} \times 3.5 ft}{.712 \times 10^{-5} \frac{ft^2}{sec}} = 24.6 \times 10^6$

It will be conservative to assume that the drag coefficient is equal to that of a sphere. (actually it must be higher)

From pg 381 of Ref 1, $C_D \approx .2$

Area = $3.37 \times 3.83 = 12.9 ft^2$
 Density = $\rho = 62.4 \#/ft^3$

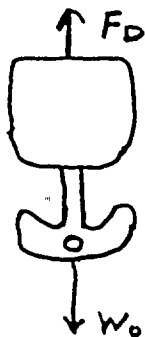
Fluid drag = $F_D = C_D \left(\frac{\rho V^2}{2g} \right)$

F_D (at time of impact with water) = $C_D \left(\frac{\rho V_0^2}{2g} \right)$
 $= \frac{.2 \times 62.4 \#/ft^3}{2 \times 32.2 \frac{ft}{sec^2}} \times 50.1^2 \frac{ft^2}{sec^2} \times 12.9 ft^2 = 6,275 \#$

Since this approaches the 8500# wt of the hook/block, the hook/block will not continue to accelerate to as high a velocity as it would in air.

It will be conservative to assume that C_D remains constant at 0.2.

$F = MA$



$(W_0 - F_D) = \frac{W}{g} \frac{d^2 x}{dt^2}$ (1)

where W_0 is the wt in water

$W_0 = W \left(\frac{\mu - 1}{\mu} \right)$ where μ is the specific wt of steel ≈ 7

$W_0 = .857 W$ (2)

$F_D = \frac{C_D \rho A}{2g} \left(\frac{dx}{dt} \right)^2$ (3)

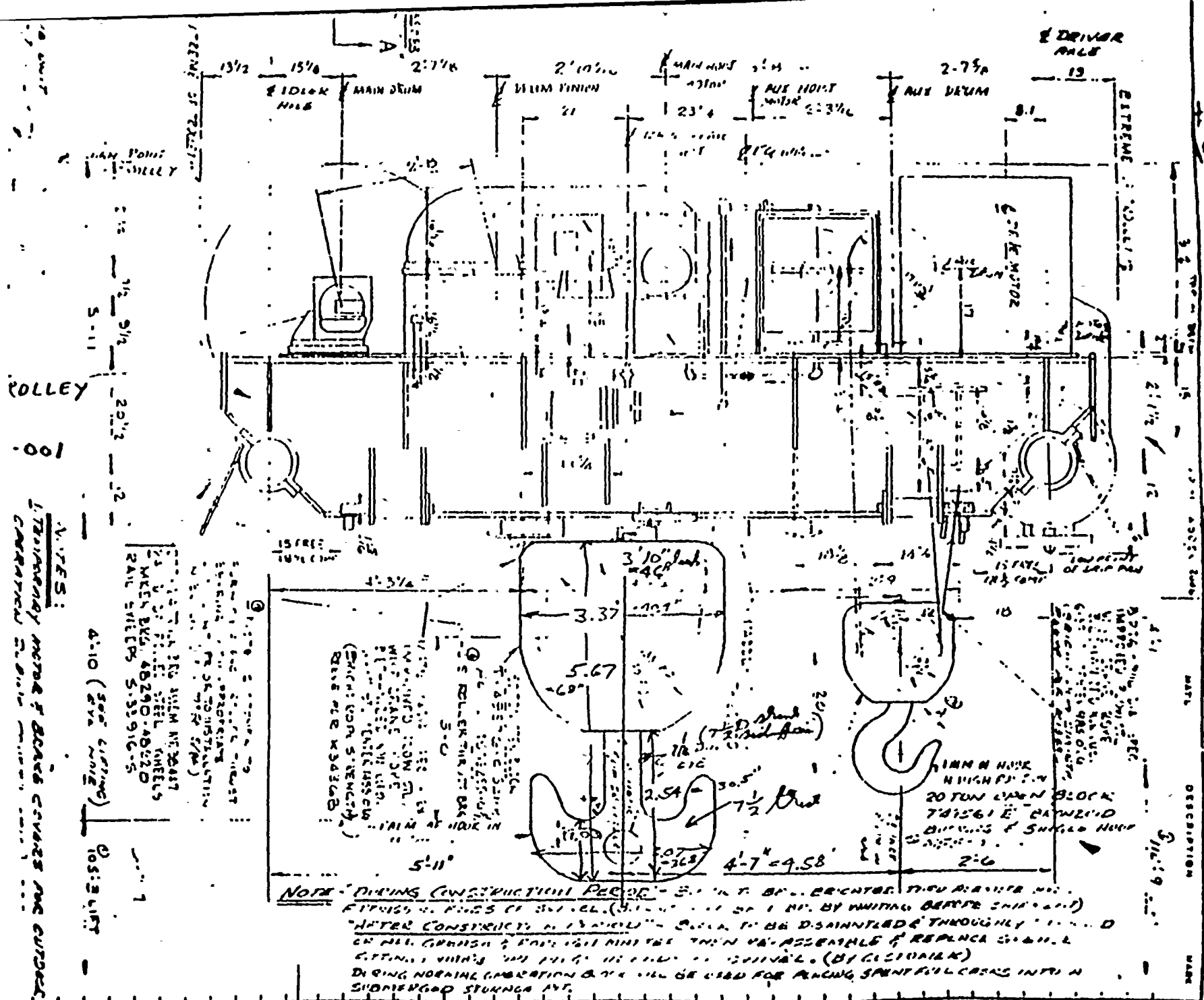
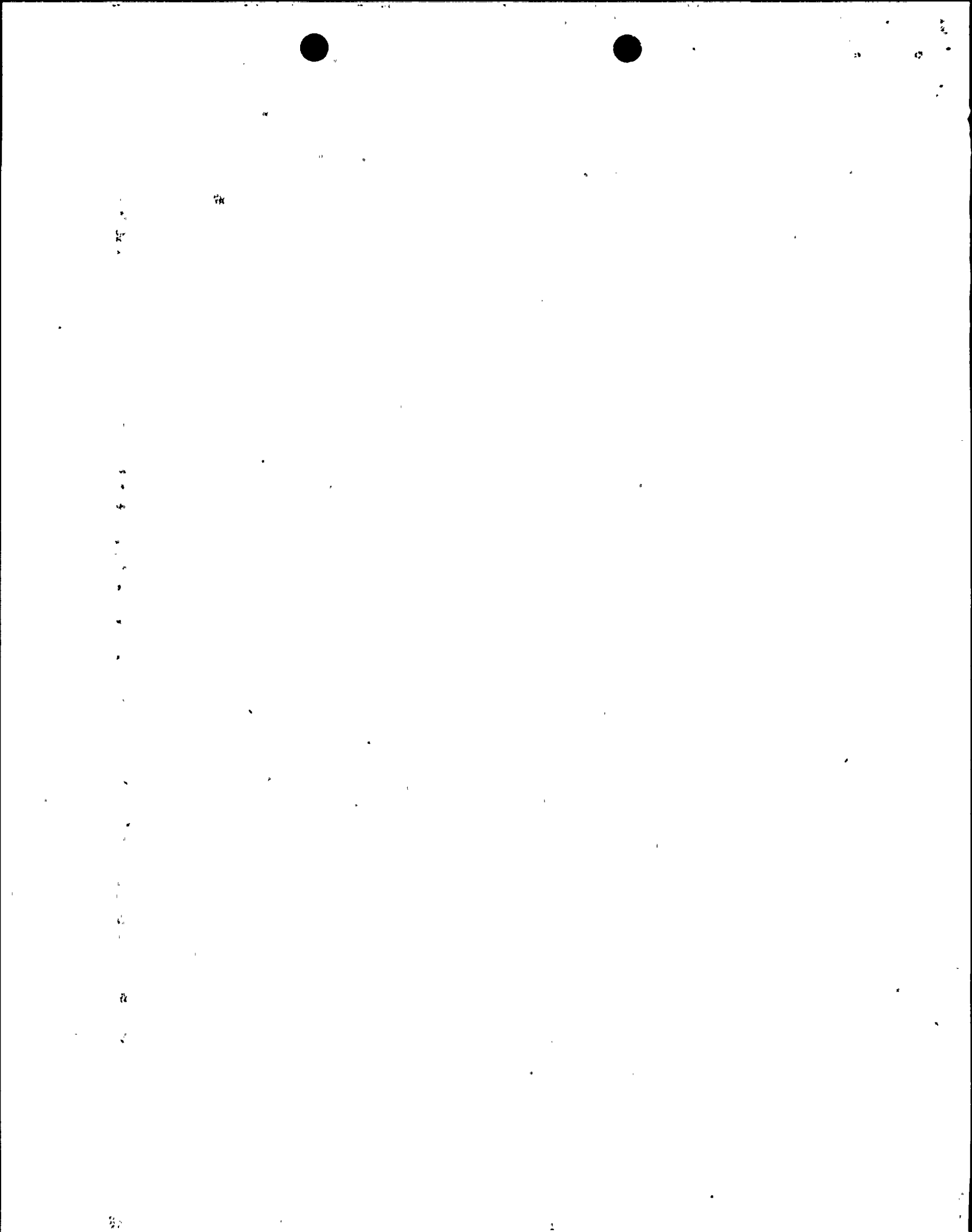


FIGURE NO. 1

$\frac{4.58}{4.27} = 1.07$

use 20.000 + mult by 1.07



drag. In the case of streamlined shapes, the frictional resistance and the resistance are of comparable values.

The dependence of the drag coefficient of shapes such as a sphere, cylinder, etc. Reynolds number is very complex (Figure 10-1). The value of c_x is maximum at very low values of Re ; decreasing with the increase of Re , passes through a first minimum at a value of $Re' \approx (2 \text{ to } 5) \times 10^3$, then increases somewhat and remains constant up to a value of $(1 \text{ to } 2) \times 10^5$ (the critical Reynolds number). It then drops sharply to a second minimum at $Re' = 5 \times 10^5$, and increases negligibly to $Re' = 10^6$, where it becomes fairly constant.

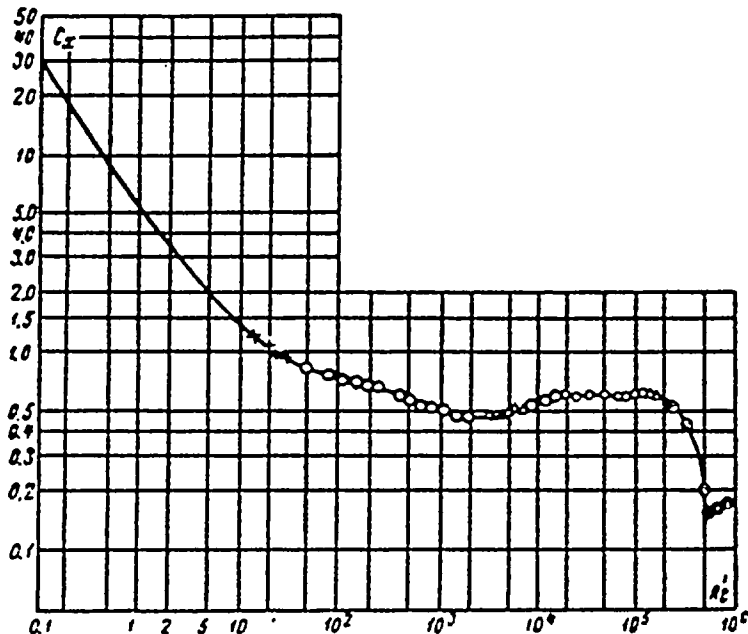
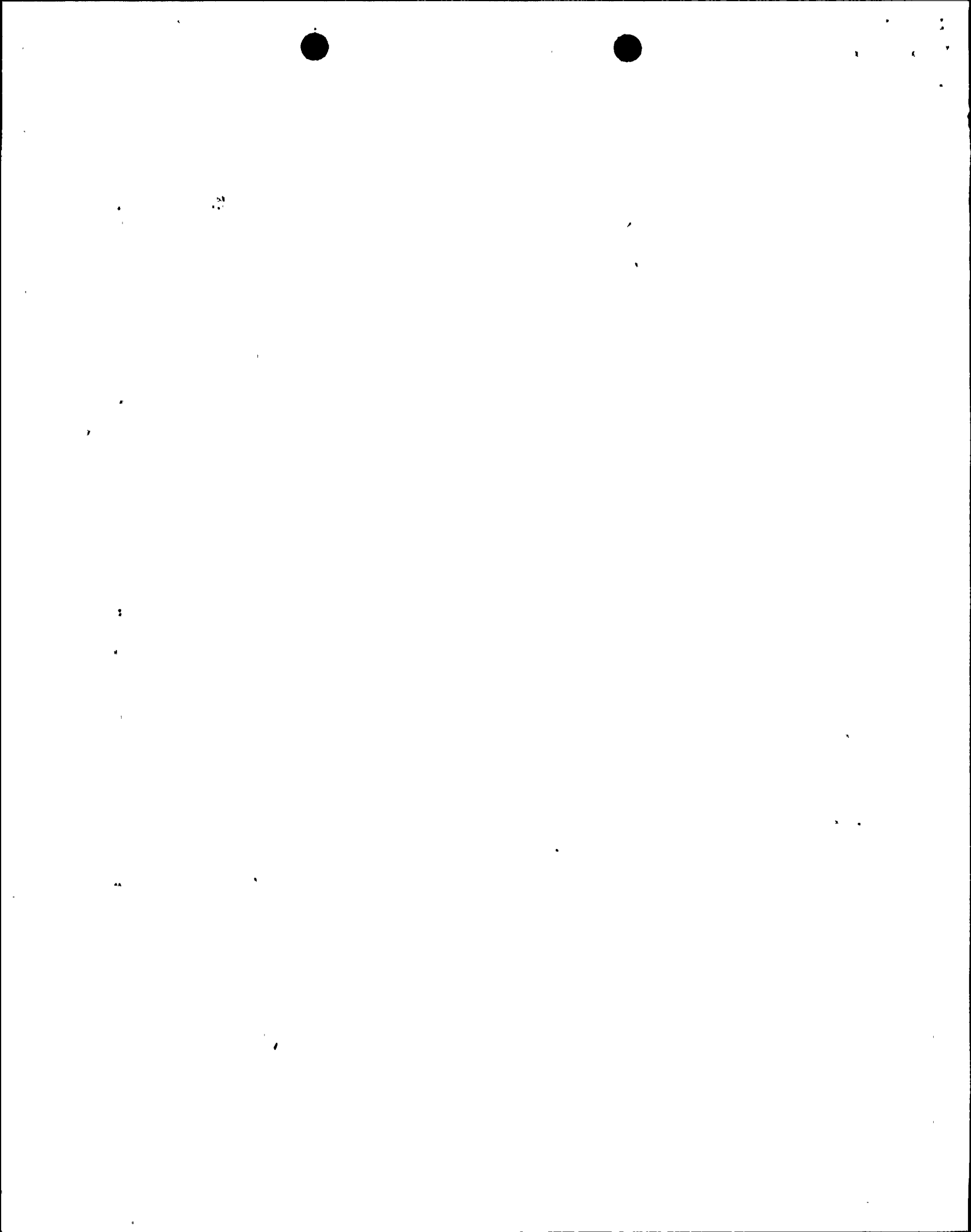


FIGURE 10-1 Drag coefficient of a sphere as a function of Reynolds number

5. The flow pattern past spheres and cylinders is characterized by the absence of eddies at small values of Re' (Figure 10-2, a). The flow is purely laminar, and the resistance of the body is determined entirely by the viscosity forces. With the increase of the value of Re' the influence of the inertia forces begins to be felt, leading to the separation of the stream from the rear of the object (Figure 10-2, b).

The stream separation here is due to the same causes as in flow in a diffuser, i. e., the increase of the pressure along the stream resulting from the decrease of velocity (Figure 10-2). Therefore, at moderate values of Re' , when the boundary layer is still laminar and is characterized by a linear distribution of the velocities, giving a maximum thickness, the stream separation from the surface of the sphere or cylinder starts almost at its widest section (Figure 10-3, a).

With the further increase of Re' , the flow in the boundary layer passes from laminar to turbulent. This is accompanied by a decrease of the boundary layer thickness, and an increased "fullness" of the velocity profile in the detached stream, which causes it to adhere again to the spherical surface. Since the inertia forces continue



Substitute (2) & (3) in (1)

$$\frac{W}{g} \frac{\partial^2 x}{\partial t^2} + \frac{C_d P A}{2g} \left(\frac{\partial x}{\partial t} \right)^2 - W_0 = 0$$

$$\frac{8,500 \#}{32.2 \frac{ft}{sec^2}} \frac{\partial^2 x}{\partial t^2} \frac{ft}{sec^2} + \frac{.2 \times 62.4 \frac{\#}{ft^3} \times 12.9 \frac{ft^2}{sec^2}}{2 \times 32.2 \frac{ft}{sec^2}} \left(\frac{\partial x}{\partial t} \right)^2 \frac{ft^2}{sec^2} - 7285 = 0$$

$$264 \frac{\partial^2 x}{\partial t^2} + 2.5 \left(\frac{\partial x}{\partial t} \right)^2 - 7285 = 0$$

$$105.6 \frac{\partial}{\partial t} \left(\frac{\partial x}{\partial t} \right) + \left(\frac{\partial x}{\partial t} \right)^2 - 2914 = 0$$

Break this into time steps of 0.1 sec and solve numerically

$$105.6 \frac{\Delta V}{.1} + V^2 - 2914 = 0$$

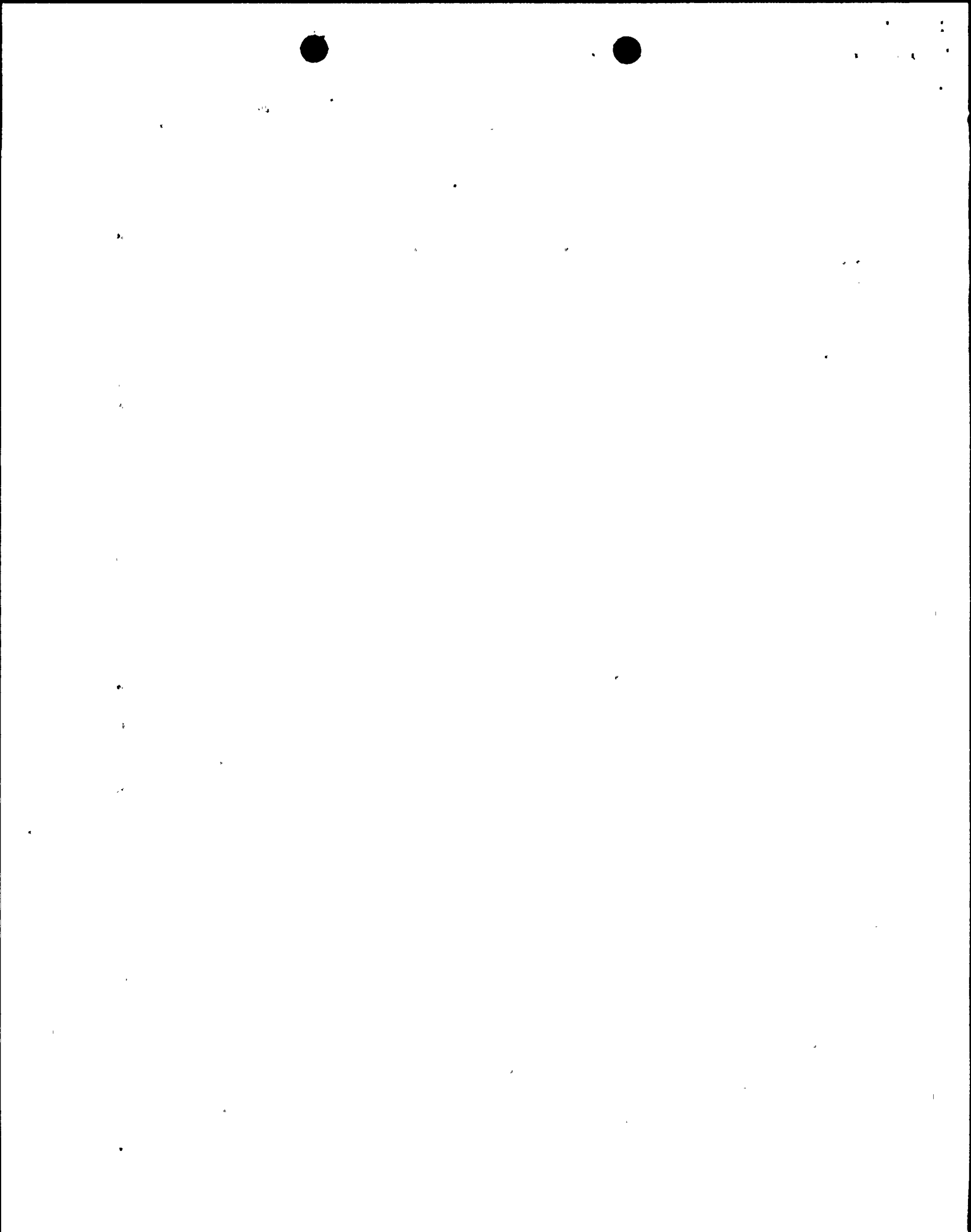
$$\Delta V = \frac{2914 - V^2}{1056}$$

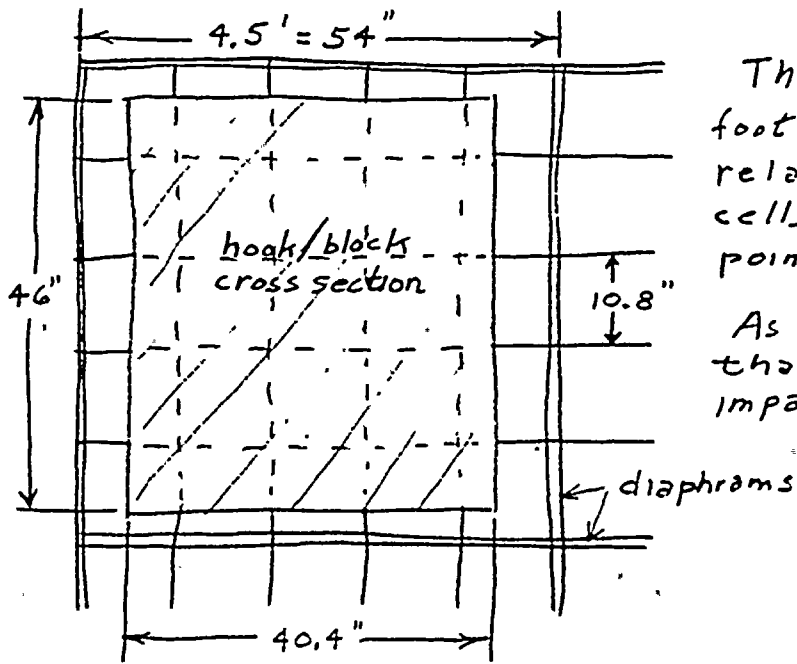
$$\Delta x = V \Delta t = 0.1 V$$

i	t (sec)	$\Delta V_i = \frac{2914 - V_{i-1}^2}{1056}$	$V_i = V_{i-1} + \Delta V_i$	$\Delta x_i = .1 V_i$	$x_i = x_{i-1} + \Delta x_i$
0	0		50.1		0
1	.1	.383	50.5	5.05	5.05
2	.2	.345	50.8	5.08	10.13
3	.3	.316	51.1	5.11	15.24
4	.4	.287	51.4	5.14	20.38
5	.5	.258	51.7	5.17	25.55

The hook impacts the rack at 23.7 ft when $V = 51.4 + \frac{(23.7 - 20.38) \cdot 3}{25.5 - 20.38}$
 $= 51.6 \text{ ft/sec}$

$$\text{Impacting energy} = \frac{WV^2}{2g} = \frac{8,500 \# \times 51.6^2 \frac{ft^2}{sec^2}}{2 \times 32.2 \frac{ft}{sec^2}} \times \frac{12.1 \frac{ft^2}{ft}}{ft} = \underline{\underline{4.22 \times 10^6 \text{ in}\#}}$$

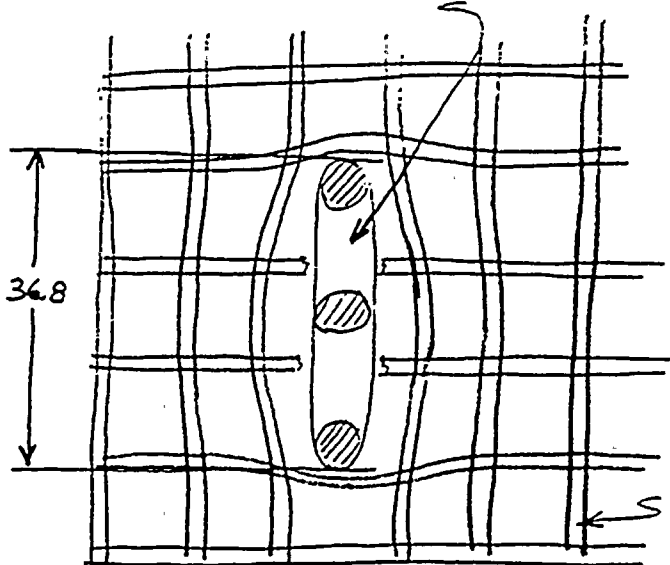




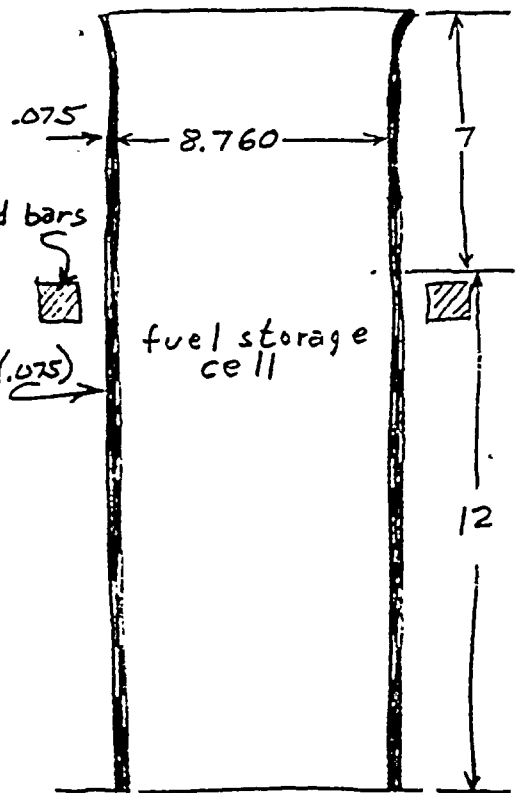
This sketch shows the footprint of the hook/block relative to the fuel storage cells for the worst possible point of impact.

As an approximation, assume that 15 fuel cells absorb the impacting energy.

hook cross section



The hook can penetrate the grid by breaking two bars and pushing two more aside.



The upper 19 inches does not contain fuel and looks as shown. This structure has a square cross section.

The hook will crush the upper 7 inches before contacting the grid bars.

We must determine how far the hook penetrates into the fuel rack in order to assess the extent of the damage. First estimate the energy absorbed by crushing the top 7 inches

Consider a flat plate as in case A1 of Table XVI from Ref 2

$$\text{buckling stress} = S' = K \frac{E}{1-\nu^2} \left(\frac{t}{b} \right)^2$$

$$a/b = 7/8.76 = .799 \quad K = 3.45 \quad \text{Note that for values of } a/b \geq .8, \text{ } K \text{ is nearly independent of } a/b$$

$$S' = \frac{3.45 \times 30 \times 10^6}{1-.287^2} \left(\frac{.075}{8.760} \right)^2 = 8,268 \text{ psi}$$

Assume that the average crushing load will occur at a stress equal to $1/3$ of this value. (see section B)

Average crushing load for the top 7 inches

$$= \frac{\substack{4 \text{ plates} \\ 4 \times 8.268 \text{ \#/in}^2}}{3} \left(\substack{\text{area of each plate} \\ (.075 \times 8.76)} \right) \text{in}^2 = 7,243 \#$$

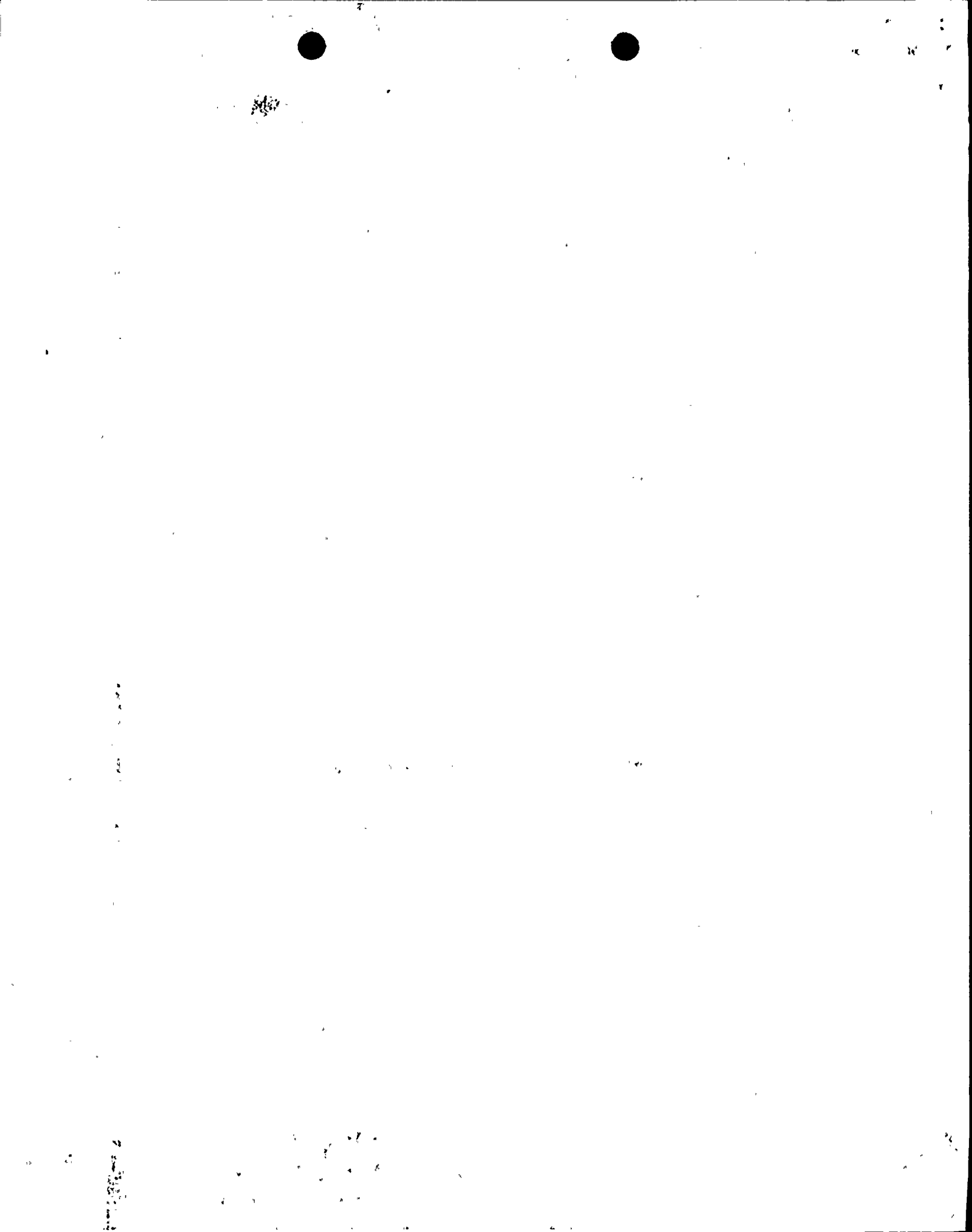
Energy absorbed in crushing the upper 7 inches of one fuel storage cell = $7,243 \# \times 7 \text{ in} = 50,700 \text{ in}\#$

From the sketch at the top of pg A-6 we see that approx 15 fuel storage cells will have the top 7 inches crushed.

$$\text{Energy absorbed} = 15 (50,700) = .760 \times 10^6 \text{ in}\#$$

$$\text{Energy left after crushing the top 7 inches of 15 cells} \\ = (4.22 - .760) \times 10^6 = \underline{\underline{3.46 \times 10^6 \text{ in}\#}}$$

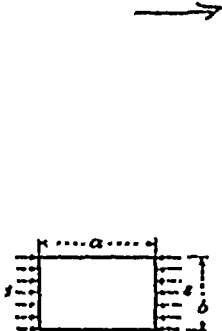
After crushing, the top 7 inches, the block will contact the grid bars. Further movement of the block will depend upon the energy absorbing capability of the inner shroud of the fuel storage cell and the grid bars. It will be conservative to assume that the grid bars absorb energy by stretching only (similar to a trampoline). Ignore the energy absorbed by bending and other local deformations.



Ref 2

TABLE XVI.—FORMULAS FOR ELASTIC STABILITY OF PLATES AND SHELLS

E = modulus of elasticity; ν = Poisson's ratio, a = longer dimension, b = shorter dimension for all rectangular plates. t = thickness for all plates and shells. All dimensions in inches, all forces in pounds, all angles in radians. Compression positive; tension negative.

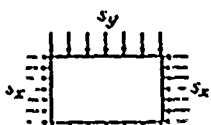
Form of plate or shell and manner of loading	Manner of support	Formulas for critical unit compressive stress σ_c , unit shear stress τ_c , load P_c , bending moment M_c , or unit external pressure p_c at which elastic buckling occurs																																		
<p>A. Rectangular plate under equal uniform compression on two opposite edges b</p> 	1. All edges simply supported	$\sigma_c = K \frac{E}{1-\nu^2} \left(\frac{t}{b}\right)^3$ <p>Here K depends on ratio $\frac{a}{b}$ and may be found from the following table:</p> <table border="1"> <tr> <td>$\frac{a}{b}$</td> <td>0.2</td> <td>0.3</td> <td>0.4</td> <td>0.6</td> <td>0.8</td> <td>1.0</td> <td>1.2</td> <td>1.4</td> <td>1.6</td> <td>1.8</td> <td>2.0</td> <td>2.2</td> <td>2.4</td> <td>2.7</td> <td>3</td> <td>∞</td> </tr> <tr> <td>K</td> <td>22.7</td> <td>10.9</td> <td>6.92</td> <td>4.23</td> <td>3.15</td> <td>2.29</td> <td>1.60</td> <td>1.16</td> <td>0.83</td> <td>0.62</td> <td>0.49</td> <td>0.40</td> <td>0.32</td> <td>0.29</td> <td>0.29</td> <td>0.29</td> </tr> </table> <p>(For unequal end compressions, see Ref. 33) (Refs. 1, 6)</p>	$\frac{a}{b}$	0.2	0.3	0.4	0.6	0.8	1.0	1.2	1.4	1.6	1.8	2.0	2.2	2.4	2.7	3	∞	K	22.7	10.9	6.92	4.23	3.15	2.29	1.60	1.16	0.83	0.62	0.49	0.40	0.32	0.29	0.29	0.29
	$\frac{a}{b}$	0.2	0.3	0.4	0.6	0.8	1.0	1.2	1.4	1.6	1.8	2.0	2.2	2.4	2.7	3	∞																			
	K	22.7	10.9	6.92	4.23	3.15	2.29	1.60	1.16	0.83	0.62	0.49	0.40	0.32	0.29	0.29	0.29																			
	2. All edges clamped	$\sigma_c = K \frac{E}{1-\nu^2} \left(\frac{t}{b}\right)^3$ <table border="1"> <tr> <td>$\frac{a}{b}$</td> <td>1</td> <td>2</td> <td>3</td> <td>∞</td> </tr> <tr> <td>K</td> <td>7.7</td> <td>0.7</td> <td>0.4</td> <td>0.73</td> </tr> </table> <p>(Refs. 1, 6, 7)</p>	$\frac{a}{b}$	1	2	3	∞	K	7.7	0.7	0.4	0.73																								
	$\frac{a}{b}$	1	2	3	∞																															
	K	7.7	0.7	0.4	0.73																															
3. Edges b simply supported, edges a clamped	$\sigma_c = K \frac{E}{1-\nu^2} \left(\frac{t}{b}\right)^3$ <table border="1"> <tr> <td>$\frac{a}{b}$</td> <td>0.4</td> <td>0.5</td> <td>0.6</td> <td>0.7</td> <td>0.8</td> <td>1.0</td> <td>1.2</td> <td>1.4</td> <td>1.6</td> <td>1.8</td> <td>2.1</td> <td>∞</td> </tr> <tr> <td>K</td> <td>7.76</td> <td>6.32</td> <td>5.80</td> <td>5.76</td> <td>6.00</td> <td>6.32</td> <td>6.80</td> <td>7.76</td> <td>8.00</td> <td>8.80</td> <td>9.76</td> <td>10.73</td> </tr> </table> <p>(Refs. 1, 6)</p>	$\frac{a}{b}$	0.4	0.5	0.6	0.7	0.8	1.0	1.2	1.4	1.6	1.8	2.1	∞	K	7.76	6.32	5.80	5.76	6.00	6.32	6.80	7.76	8.00	8.80	9.76	10.73									
$\frac{a}{b}$	0.4	0.5	0.6	0.7	0.8	1.0	1.2	1.4	1.6	1.8	2.1	∞																								
K	7.76	6.32	5.80	5.76	6.00	6.32	6.80	7.76	8.00	8.80	9.76	10.73																								
4. Edges b simply supported, one edge a simply supported, other edge a free	$\sigma_c = K \frac{E}{1-\nu^2} \left(\frac{t}{b}\right)^3$ <table border="1"> <tr> <td>$\frac{a}{b}$</td> <td>0.5</td> <td>1.0</td> <td>1.2</td> <td>1.4</td> <td>1.6</td> <td>1.8</td> <td>2.0</td> <td>2.5</td> <td>3.0</td> <td>4.0</td> <td>5.0</td> </tr> <tr> <td>K</td> <td>3.62</td> <td>1.18</td> <td>0.934</td> <td>0.784</td> <td>0.647</td> <td>0.622</td> <td>0.674</td> <td>0.802</td> <td>0.464</td> <td>0.425</td> <td>0.416</td> </tr> </table> <p>(Ref. 1)</p>	$\frac{a}{b}$	0.5	1.0	1.2	1.4	1.6	1.8	2.0	2.5	3.0	4.0	5.0	K	3.62	1.18	0.934	0.784	0.647	0.622	0.674	0.802	0.464	0.425	0.416											
$\frac{a}{b}$	0.5	1.0	1.2	1.4	1.6	1.8	2.0	2.5	3.0	4.0	5.0																									
K	3.62	1.18	0.934	0.784	0.647	0.622	0.674	0.802	0.464	0.425	0.416																									
5. Edges b simply supported, one edge a clamped, other edge a free	$\sigma_c = K \frac{E}{1-\nu^2} \left(\frac{t}{b}\right)^3$ <table border="1"> <tr> <td>$\frac{a}{b}$</td> <td>1</td> <td>1.1</td> <td>1.2</td> <td>1.3</td> <td>1.4</td> <td>1.6</td> <td>1.6</td> <td>1.7</td> <td>1.8</td> <td>1.9</td> <td>2.0</td> <td>2.2</td> <td>2.4</td> </tr> <tr> <td>K</td> <td>1.40</td> <td>1.24</td> <td>1.21</td> <td>1.16</td> <td>1.12</td> <td>1.10</td> <td>1.09</td> <td>1.09</td> <td>1.10</td> <td>1.12</td> <td>1.14</td> <td>1.19</td> <td>1.21</td> </tr> </table> <p>(Ref. 1)</p>	$\frac{a}{b}$	1	1.1	1.2	1.3	1.4	1.6	1.6	1.7	1.8	1.9	2.0	2.2	2.4	K	1.40	1.24	1.21	1.16	1.12	1.10	1.09	1.09	1.10	1.12	1.14	1.19	1.21							
$\frac{a}{b}$	1	1.1	1.2	1.3	1.4	1.6	1.6	1.7	1.8	1.9	2.0	2.2	2.4																							
K	1.40	1.24	1.21	1.16	1.12	1.10	1.09	1.09	1.10	1.12	1.14	1.19	1.21																							
6. Edges b clamped, edges a simply supported	$\sigma_c = K \frac{E}{1-\nu^2} \left(\frac{t}{b}\right)^3$ <table border="1"> <tr> <td>$\frac{a}{b}$</td> <td>0.6</td> <td>0.8</td> <td>1.0</td> <td>1.2</td> <td>1.4</td> <td>1.6</td> <td>1.7</td> <td>1.8</td> <td>2.0</td> <td>2.6</td> <td>3.0</td> </tr> <tr> <td>K</td> <td>11.0</td> <td>7.18</td> <td>5.64</td> <td>4.80</td> <td>4.48</td> <td>4.39</td> <td>4.39</td> <td>4.26</td> <td>3.99</td> <td>3.72</td> <td>3.63</td> </tr> </table> <p>(Ref. 1)</p>	$\frac{a}{b}$	0.6	0.8	1.0	1.2	1.4	1.6	1.7	1.8	2.0	2.6	3.0	K	11.0	7.18	5.64	4.80	4.48	4.39	4.39	4.26	3.99	3.72	3.63											
$\frac{a}{b}$	0.6	0.8	1.0	1.2	1.4	1.6	1.7	1.8	2.0	2.6	3.0																									
K	11.0	7.18	5.64	4.80	4.48	4.39	4.39	4.26	3.99	3.72	3.63																									

312

FORMULAS FOR STRESS AND STRAIN (CONT'D.)

A-8

B. Rectangular plate under uniform compression (or tension) σ_x on edges b and uniform compression (or tension) σ_y on edges a



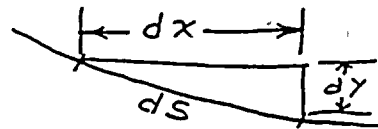
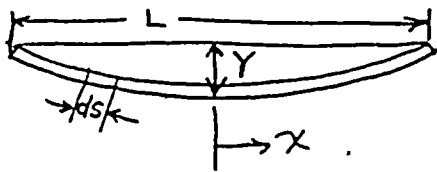
7. All edges simply supported

$$\sigma_c = \frac{m^2}{a^2} + \frac{n^2}{b^2} - 0.823 \frac{E}{1-\nu^2} \left(\frac{m^2}{a^2} + \frac{n^2}{b^2}\right)$$

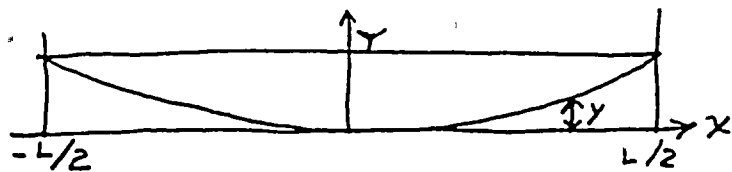
Here m and n signify the number of half-waves in the buckled plate in the x and y directions, respectively. To find σ_c for a given σ_x , take $m = 1, n = 1$ if: $C \left(1 - \frac{a^2}{b^2}\right) < \sigma_x < C \left(b + \frac{a^2}{b^2}\right)$, where $C = \frac{0.823 E t^2}{(1-\nu^2) a^2}$. If σ_x is too large to satisfy this inequality, take $n = 1$ and m to satisfy: $C \left(2m^2 - 2m + 1 + \frac{a^2}{b^2}\right) < \sigma_x < C \left(2m^2 + 2m + 1 + \frac{a^2}{b^2}\right)$. If σ_x is too small to satisfy this inequality, take $m = 1$ and n to satisfy: $C \left[1 - n^2(n-1) \frac{a^2}{b^2}\right] > \sigma_x > C \left[1 - n^2(n+1) \frac{a^2}{b^2}\right]$ (Refs. 1, 6)

ART. 50

Determine the relationship between the center deflection and the strain in the grid bars.



$$ds = \sqrt{(dx)^2 + (dy)^2} = \sqrt{1 + \left(\frac{dy}{dx}\right)^2} dx$$



Assume each bar takes a quadratic shape

$$y = C_1 x^2 + C_2 x$$

$$\frac{dy}{dx} = 2C_1 x + C_2$$

When $x=0$, $\frac{dy}{dx} = 0$ Therefore $C_2 = 0$

When $x=L/2$, $y=Y$ $Y = \frac{C_1 L^2}{4}$ or $C_1 = \frac{4Y}{L^2}$

$$y = 4Y \left(\frac{x}{L}\right)^2 \quad \text{deflection} = Y - y = Y \left[1 - 4\left(\frac{x}{L}\right)^2\right]$$

$$\frac{dy}{dx} = \frac{8Yx}{L^2} \quad ds = \sqrt{1 + \frac{64Y^2 x^2}{L^4}} dx$$

$$\text{Elongated length} = 2 \int_0^{L/2} ds = 2 \int_0^{L/2} \sqrt{1 + c^2 x^2} dx$$

$$\text{where } c = 8Y/L^2$$

To simplify the integration, let $z = cx$, $dz = c dx$

For the upper limit, when $x=L/2$, $z = cL/2$

$$\text{Elongated length} = \frac{z}{c} \int_0^{\frac{cL}{2}} \sqrt{1+z^2} dz$$

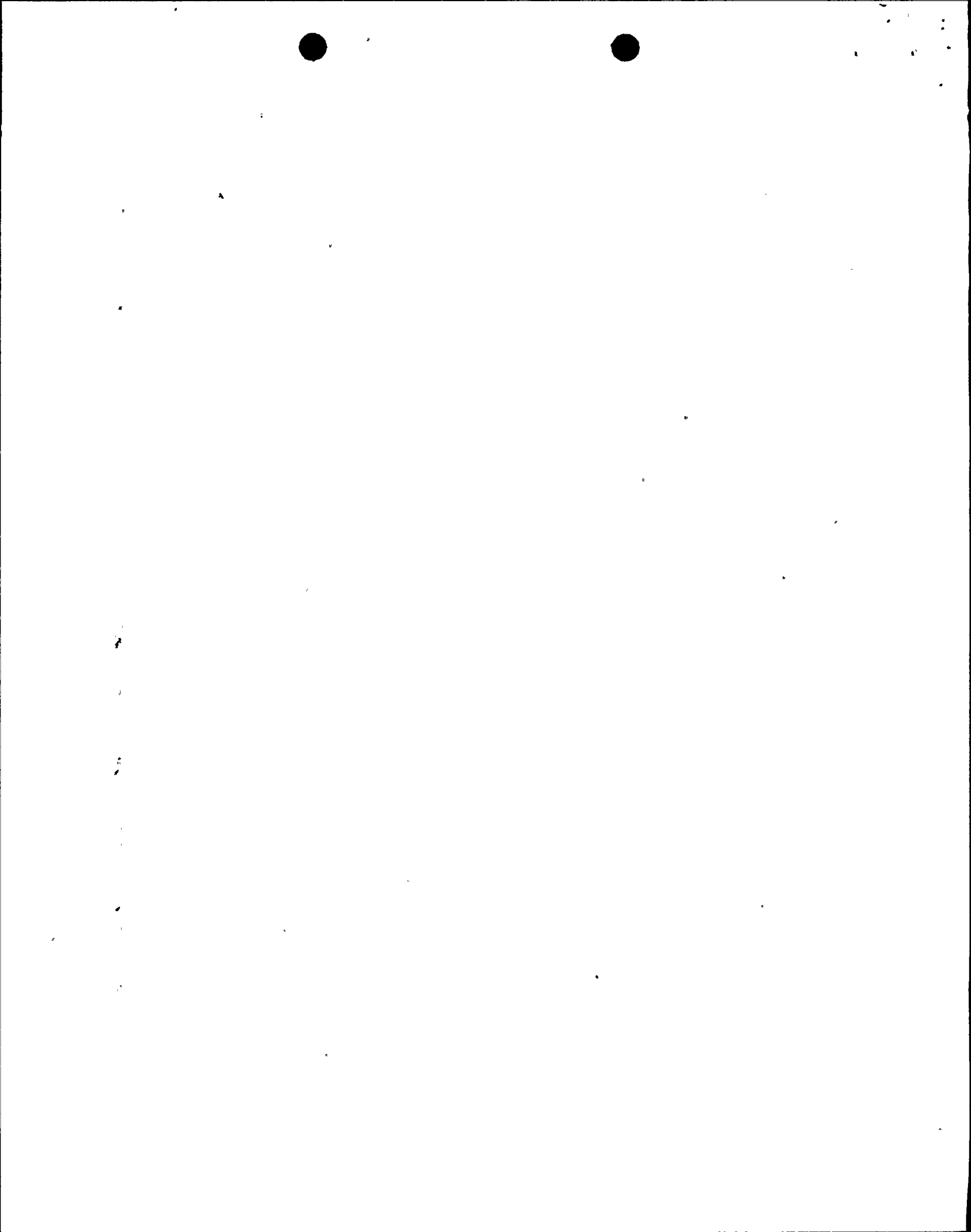
$$= \frac{1}{c} \left[z \sqrt{1+z^2} + \ln(z + \sqrt{z^2+1}) \right] \quad \left(\text{From case 124 of } \begin{array}{l} \text{'Table of Integrals', Pierce} \\ \text{ } \end{array} \right)$$

$$= \frac{1}{c} \left[\frac{cL}{2} \sqrt{1 + \left(\frac{cL}{2}\right)^2} + \ln\left(\frac{cL}{2} + \sqrt{1 + \left(\frac{cL}{2}\right)^2}\right) \right]$$

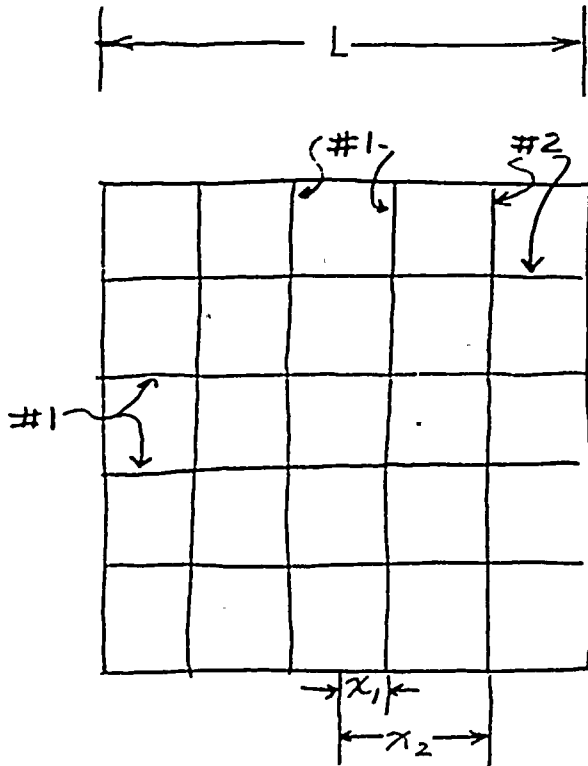
$$= \frac{L^2}{8Y} \left[\frac{4Y}{L} \sqrt{1 + \left(\frac{4Y}{L}\right)^2} + \ln\left(\frac{4Y}{L} + \sqrt{1 + \left(\frac{4Y}{L}\right)^2}\right) \right]$$

$$\text{Let } \frac{4Y}{L} = \delta$$

$$\text{Extention of bar} = \frac{L^2}{8Y} \left[\delta \sqrt{1 + \delta^2} + \ln(\delta + \sqrt{1 + \delta^2}) \right] - L$$



$$A = 11$$



$$L = 54 \text{ in}$$

let Y_0 = deflection at center of grid

let Y_1 = deflection at center of bars #1
 Y_2 = " " " " " " #2

$$\frac{x_1}{L} = \frac{.5}{5} = .1$$

$$Y_1 = Y_0 [1 - 4(.1)^2] = .96 Y_0$$

$$\delta_1 = \frac{4}{5^4} (.96 Y_0) = .0711 Y_0$$

$$\frac{x_2}{L} = \frac{1.5}{5} = .3$$

$$Y_2 = Y_0 [1 - 4(.3)^2] = .64 Y_0$$

$$\delta_2 = \frac{4}{5^4} (.64 Y_0) = .0474 Y_0$$

$$\begin{aligned} \text{Extension of bar \#1} &= \frac{54^2}{8(.96 Y_0)} \left[.0711 Y_0 \sqrt{1 + (.0711 Y_0)^2} + \ln(.0711 Y_0 + \sqrt{1 + (.0711 Y_0)^2}) \right] - 54 \\ &= 27.00 \sqrt{1 + (.0711 Y_0)^2} + \frac{379.7}{Y_0} \ln(.0711 Y_0 + \sqrt{1 + (.0711 Y_0)^2}) - 54 \end{aligned}$$

$$\begin{aligned} \text{Extension of bar \#2} &= \frac{54^2}{8(.64 Y_0)} \left[.0474 Y_0 \sqrt{1 + (.0474 Y_0)^2} + \ln(.0474 Y_0 + \sqrt{1 + (.0474 Y_0)^2}) \right] - 54 \\ &= 27.00 \sqrt{1 + (.0474 Y_0)^2} + \frac{569.5}{Y_0} \ln(.0474 Y_0 + \sqrt{1 + (.0474 Y_0)^2}) - 54 \end{aligned}$$

In order to calculate the energy absorbed by these bars, it is necessary to determine the area under the curve of force vs deflection. The ordinary stress-strain for 304 S.S. cannot be used since the stress is obtained by dividing the force as measured in the tensile machine by the original cross sectional area of the tensile specimen. This is acceptable for design applications where failure is to be avoided. However, for this application where gross deformations are involved, a curve of true stress vs true strain for 304 S.S. is required.

Determine the energy absorbing capability of the grid bars

From Reference 3, pg 200,

$$\text{True strain} = \epsilon = \ln(1 + \text{elongation})$$

From pg 200, (attached) the true stress vs true strain is shown for 301 S.S. As an example, the deformation work is shown for the case where the true strain is 0.56 ⁱⁿ/_{in}

For 301 SS, $\epsilon_t = 1.25$ ⁱⁿ/_{in}
 $\sigma_u = 185,000$ psi
 $\sigma_y = 48,000$ psi

The rack is constructed with 304 SS. Unfortunately, a true stress vs true strain curve has not been found for 304 SS. Assume that the true stress and true strain properties of the two materials may be related in the same way as conventionally measured properties

From pg 384 of Ref 1,

	301 SS (annealed plates)	304 SS (annealed plates)
Tensile Strength, psi	105,000	82,000 (bars are 85,000)
Yield Strength	40,000	35,000
Elongation	55%	60%

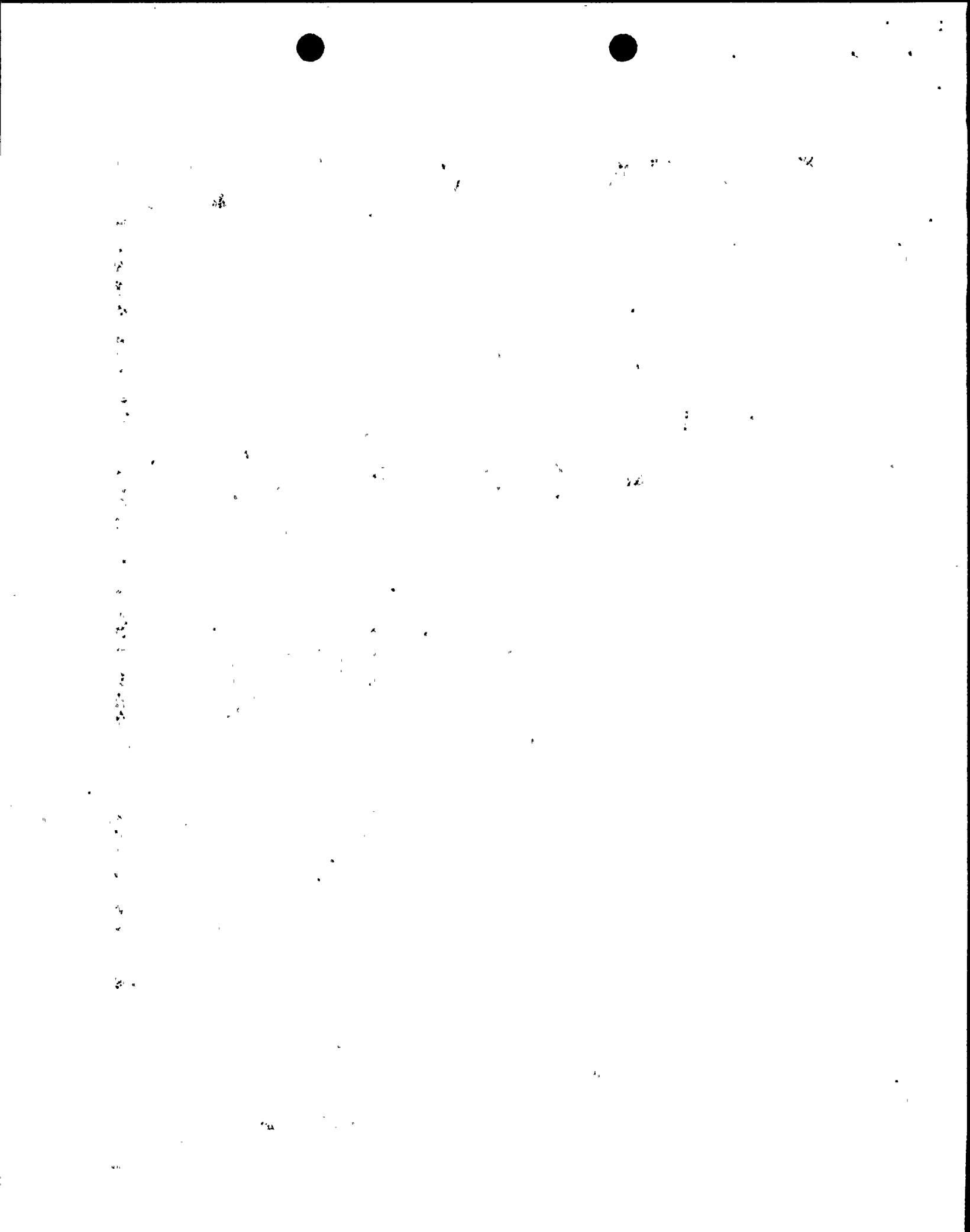
For 304 SS,

$$\epsilon_t = 1.25 \left(\frac{60}{55} \right) = 1.36 \text{ } ^{\text{in}}/\text{in}$$

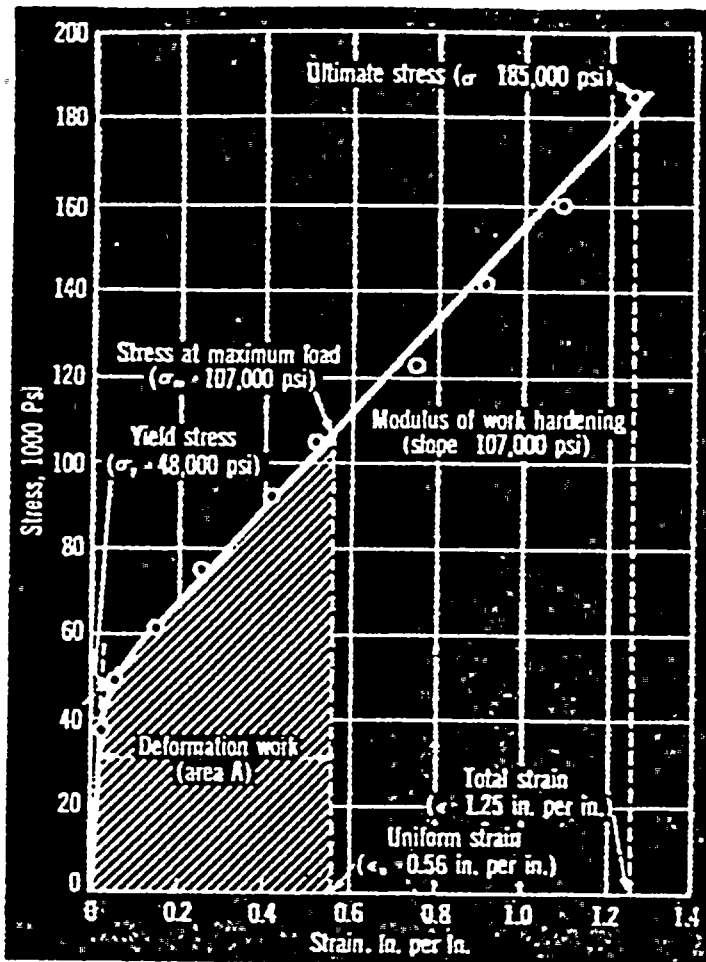
$$\sigma_u = 185,000 \left(\frac{82,000}{105,000} \right) = 144,500 \text{ psi}$$

$$\sigma_y = 48,000 \left(\frac{35,000}{40,000} \right) = 42,000 \text{ psi}$$

Use the properties of annealed plates even though the values for bars would be slightly higher.



Ref 3



True stress-true strain tensile plot shows factors which are important in an analysis of press formability.

of load. It is related to elongation in the following manner:

$$\epsilon = \ln(1 + \text{elongation})$$

The graph shows a true stress-true strain tensile curve for type 301 stainless steel strip. This plot differs from a nominal tensile plot in that the former is corrected for the constantly changing specimen dimensions which occur during testing, while the latter is plotted using original specimen dimensions. The "true" test is therefore a more accurate indication of the performance of a material during deformation.

The true stress-true strain tensile properties which are significant in an analysis of press formability (shown in the graph) include:

- Yield Stress (σ_y) – The stress at which a specimen shows deviation from straight line proportionality of stress to strain.
- Stress at Maximum Load (σ_m) – The stress at the highest load (in pounds) sustained by the specimen.
- Maximum Uniform Strain (ϵ_u) – Maximum value of straining before uniform deformation ceases and localized deformation and necking take place. This is the strain at point of maximum load.
- Modulus of Work Hardening – Slope of the plastic region of the true stress-true strain curve. Modulus indicates rate of cold work hardening.
- Deformation Work (A) – Area under true stress-true strain curve to point of maximum load. This is a measure of the work (in inch-pounds) required to elongate the tensile specimen through the region of uniform strain.

True Stress-True Strain Tensile Test

The true stress-true strain tensile test is a plot of the stress (σ) applied to a specimen versus the specimen strain (ϵ) for each stress level. True stress is the load on the specimen divided by the cross sectional area of the specimen at that load. True strain is the deformation which occurs at each increment

results of any value in a study of press formability (see box above).

The Formability Factor

Maximum uniform strain is the most important factor in press formability. A stainless steel blank can be formed as long as every area is deforming uniformly. As soon

as the strain in any section of the steel surpasses the maximum uniform strain, localized necking will occur at that point, leading to rupture. Total strain (or elongation) in a tensile specimen is unsatisfactory as an indicator of press formability, since only an undetermined amount of total "stretch" is uniform.

However, factors other than uniform strain

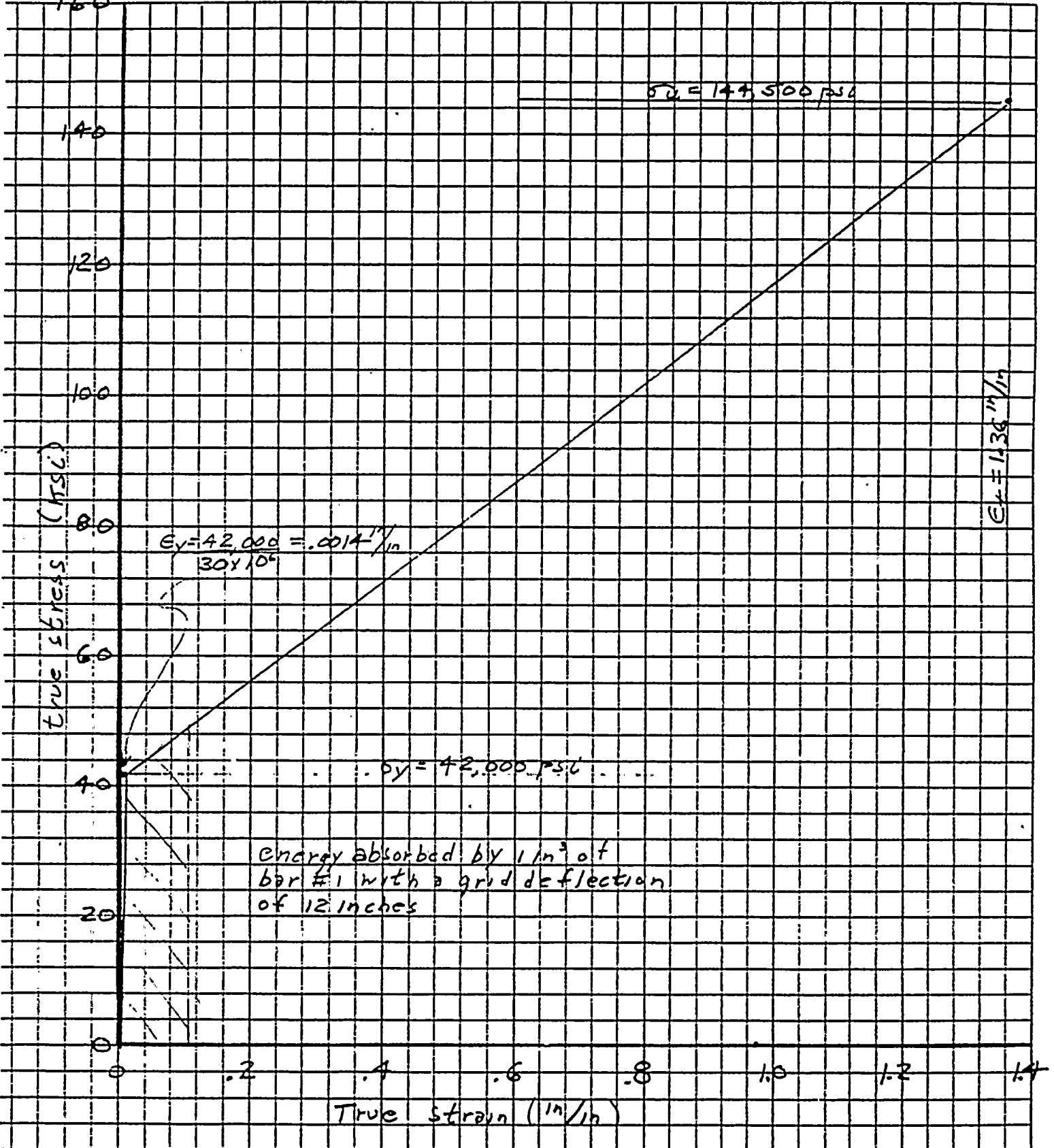
Ref 3

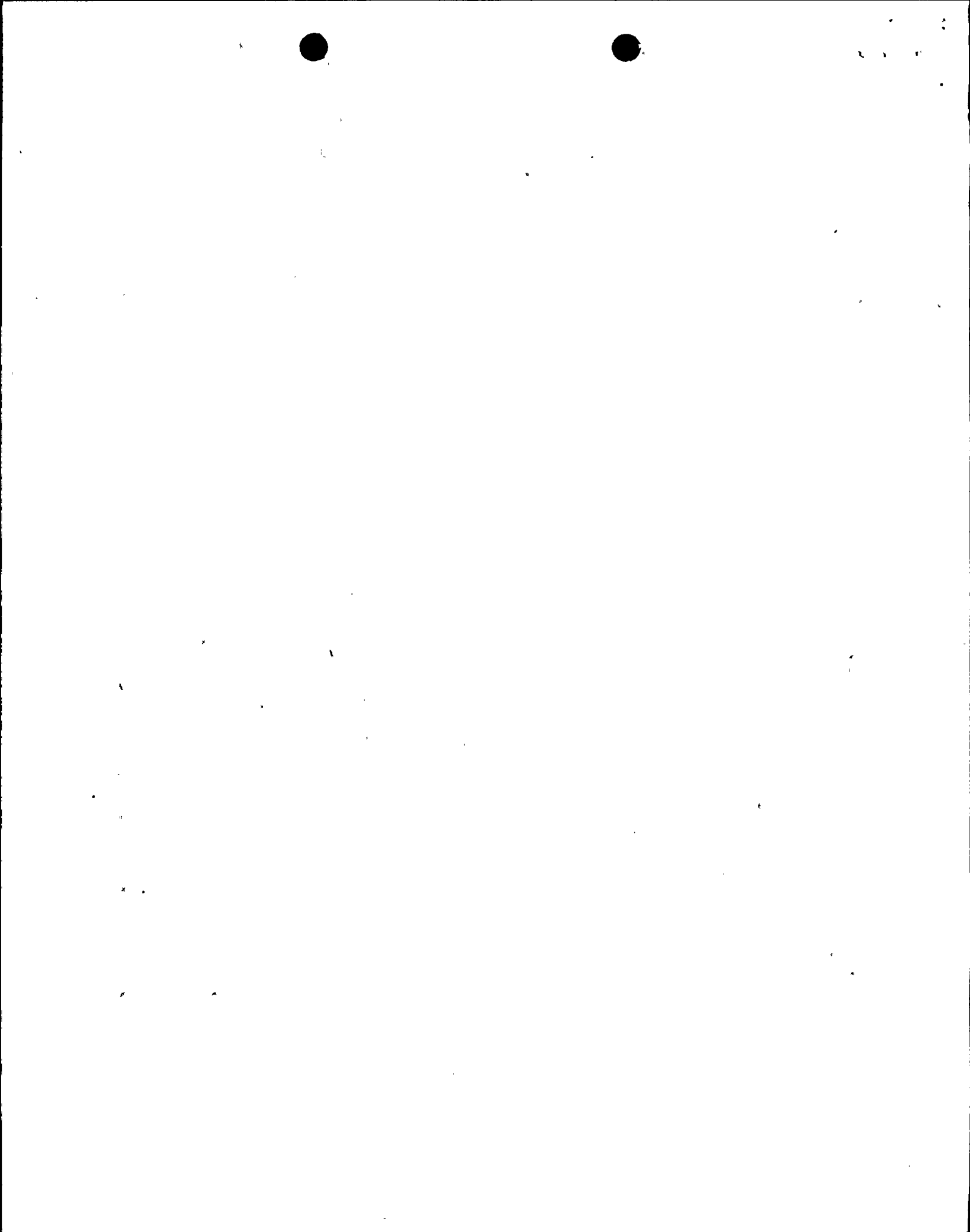
Standard Stainless and Heat-Resisting Steels

AISI Type (UNS)	Typical Composition, % (a)	Form (b)	Mechanical Properties of Annealed Material at Room Temperature				Nominal Properties of Annealed Material at Low Temperature					
			Tensile Strength, 10 ³ psi	Yield Strength, 10 ³ psi	Elongation, %	Hardness	Temperature, F	Tensile Strength, 10 ³ psi	Yield Strength, 10 ³ psi	Elongation, %	Reduction in Area, %	120° Impact Energy, ft-lb
201 (S20100)	16-18 Cr, 3.5-5.5 Ni, 0.15 C, 5.5-7.5 Mn, 1.0 Si, 0.060 P, 0.030 S, 0.25 N	Sheets	115	55	55	Rb 90	-70 -300	—	—	—	—	110 38
		Strips	115	55	55	Rb 90						
		Tubing	115	55	55	Rb 90						
202 (S20200)	17-19 Cr, 4-6 Ni, 0.15 C, 7.5-10.0 Mn, 1.0 Si, 0.060 P, 0.030 S, 0.25 N	Sheets	105	55	55	Rb 90	-70 -100 -300 -423	100 145 200 220	55 95 150 170	55 38 15 5	—	110 — 42
		Strips	105	55	55	Rb 90						
		Tubing	105	55	55	Rb 90						
205 (S20500)	16.5-18 Cr, 1-1.75 Ni, 0.12-0.25 C, 14-15.5 Mn, 1.0 Si, 0.060 P, 0.030 S, 1-1.75 Mo, 0.32-0.40 N	Plates	120	69	58	Rb 98	—	—	—	—	—	200(e)
301 (S30100)	16-18 Cr, 6-8 Ni, 0.15 C, 2.0 Mn, 1.0 Si, 0.045 P, 0.030 S	Plates	105	40	55	Bhn 165	-70 -32 -40 -80 -275	105 155 180 195 275	40 43 48 50 75	60 53 42 40 30	70 64 63 62 57	100 110 110 110 110
		Sheets	110	40	60	Rb 85						
		Strips	110	40	60	Rb 85						
		Tubing	105	40	50	Rb 85						
302 (S30200)	17-19 Cr, 8-10 Ni, 0.15 C, 2.0 Mn, 1.0 Si, 0.045 P, 0.030 S	Bars	85	35	60	Bhn 150	-70 -32 -40 -80 -120 -423	94 122 145 161 219 250	37 40 48 50 68 125	68 65 60 57 46 41	78 76 73 70 70 55	110 110 110 110 110 —
		Plates	90	35	60	Rb 80						
		Sheets	90	40	50	Rb 85						
		Strips	90	40	50	Rb 85						
		Tubing	85	35	50	Rb 85						
		Wire	90	35	60	Rb 83						
302B (S30215)	17-19 Cr, 8-10 Ni, 0.15 C, 2.0 Mn, 2.0-3.0 Si, 0.045 P, 0.030 S	Bars	90	40	50	Rb 85	-70	Not applicable. Silicon added to type 302 for oxidation resistance				90
		Plates	90	40	50	Rb 85						
		Sheets	95	40	55	Rb 85						
		Strips	95	40	55	Rb 85						
303 (S30300)	17-19 Cr, 8-10 Ni, 0.15 C, 2.0 Mn, 1.0 Si, 0.20 P, 0.15 S min, 0.60 Mo (optional)	Bars	90	35	50	Bhn 160	-70 -32 -40 -80 -320 -452	100 114 145 162 235 267	40 40 40 40 37 —	67 61 45 40 35 30	67 65 62 60 52 37	85 90 100 106 125 —
		Tubing	80	38	52							
303S4 (S30323)	17-19 Cr, 8-10 Ni, 0.15 C, 2.0 Mn, 1.0 Si, 0.20 P, 0.060 S, 0.15 S4 min	Wire	90	35	50							
			90	35	50							
304 (S30400)	18-20 Cr, 8-10.5 Ni, 0.08 C, 2.0 Mn, 1.0 Si, 0.045 P, 0.030 S	Bars	85	35	60	Bhn 149	-70 -32 -40 -80 -120 -423	95 130 155 170 221 243	35 34 34 39 40 50	65 55 47 39 40 40	71 68 64 63 55 50	110 110 110 110 110 110
		Plates	82	35	60	Bhn 149						
		Sheets	84	42	55	Rb 80						
		Strips	84	42	55	Rb 80						
		Tubing	85	35	60	Rb 80						
304L (S30403)	18-20 Cr, 8-12 Ni, 0.03 C, 2.0 Mn, 1.0 Si, 0.045 P, 0.030 S	Plates	79	33	60	Bhn 143	-70 -32 -40 -80 -120 -423	170 221 243	34 39 40 50	39 40 40	55 50	110 110
		Sheets	81	39	55	Rb 79						
(S30430)	17-19 Cr, 8-10 Ni, 0.08 C, 2.0 Mn, 1.0 Si, 0.045 P, 0.030 S, 3-4 Cu	Wire	73	31	70	Rb 70	—	—	—	—	—	240(e)
			73	31	70	Rb 70	—	—	—	—	—	240(e)
304N (S30451)	18-20 Cr, 8-10.5 Ni, 0.08 C, 2.0 Mn, 1.0 Si, 0.045 P, 0.030 S, 0.10-0.16 N	Bars	90	42	55	Bhn 180	—	—	—	—	—	—
305 (S30500)	17-19 Cr, 10.50-13 Ni, 0.12 C, 2.0 Mn, 1.0 Si, 0.045 P, 0.030 S	Plates	85	35	55	—	-70	—	—	—	—	110
		Sheets	85	38	50	Rb 80						
		Strips	85	38	50	Rb 80						
		Tubing	80	36	56	Rb 80						
		Wire	85	34	60	Rb 77						
308 (S30800)	19-21 Cr, 10-12 Ni, 0.08 C, 2.0 Mn, 1.0 Si, 0.045 P, 0.030 S	Bars	85	30	55	Rb 80	-70	—	—	—	—	110
		Plates	85	30	55	Bhn 150						
		Sheets	85	35	50	Rb 80						
		Strips	85	35	50	Rb 80						
		Tubing	85	35	50	Rb 80						
		Wire	95(f)	60(f)	50(f)	Rb 80						

(a) Single values are maximums, except as noted, (b) Forms listed are only those for which mechanical properties are given. Most types are available in many forms; (c) Austenitic, hardenable by cold working, not hardenable by heat treatment. Ferritic: not hardenable by heat treatment or cold working. Martensitic, hardenable by heat treatment; (d) Followed by rapid cooling. H is hardening temperature. T is tempering; (e) Charpy V notch; (f) Soft temper; (g) Composition for type 310 tubing varies slightly from AISI values, for standard compositions, refer to ASTM A213; (h) Stabilizing temperature, 1550 to 1650 F; (i) Retarded cool; (j) Full anneal, followed by slow cooling; (k) Low anneal; (l) Tempering within the range of 800 to 1100 F is not recommended because of resulting low and erratic impact properties and reduced corrosion resistance. Time at temperature and temperatures may vary depending on part size; (m) Retarded cool and anneal; (n) Mechanical properties are for a solution treated condition. Source: Committee of Stainless Steel Producers, American Iron and Steel Institute.

True Stress vs True Strain for 304 S.S.





Suppose the block crushes the top 19 inches of the fuel storage cell. The deflection at the center of the grid is then $19 - 7 = 12$ inches

From pg A-7, Average crushing load = 7,243 #
15

Energy spent in crushing the fuel storage cells

$$= 7,243 \times 15 \times 19 = 2.06 \times 10^6 \text{ in}\#$$

$$\text{Energy left} = (4.22 - 2.06) \times 10^6 = \underline{2.16 \times 10^6 \text{ in}\#}$$

From pg A-11, with $Y_0 = 12$,

$$\begin{aligned} \text{Extension of bar \#1} &= 5.97 \text{ in} & \text{volume of each bar} &= 1.25^2 (54) \\ \text{Extension of bar \#2} &= 2.78 & &= 84.4 \text{ in}^3 \end{aligned}$$

$$\begin{aligned} \text{Elongation of bar \#1} &= 5.97 / 54 = .1106 \text{ in/in} \\ \text{" " " \#2} &= 2.78 / 54 = .0515 \end{aligned}$$

$$\begin{aligned} \text{True strain of bar \#1} &= \ln(1 + .1106) = .105 \\ \text{\#2} &= \ln(1 + .0515) = .0502 \end{aligned}$$

$$\text{True stress in bar \#1} \approx 42,000 + \frac{.105}{1.36} (144,500 - 42,000) = 49,914 \text{ psi}$$

Energy absorbed by four bars \#1 (see page A-15)

$$= 4 \times 84.4 \text{ in}^3 \left[\frac{42,000 + 49,914}{2} \right] \frac{\#}{\text{in}^2} \times .105 \frac{\text{in}}{\text{in}} = 1.63 \times 10^6 \text{ in}\#$$

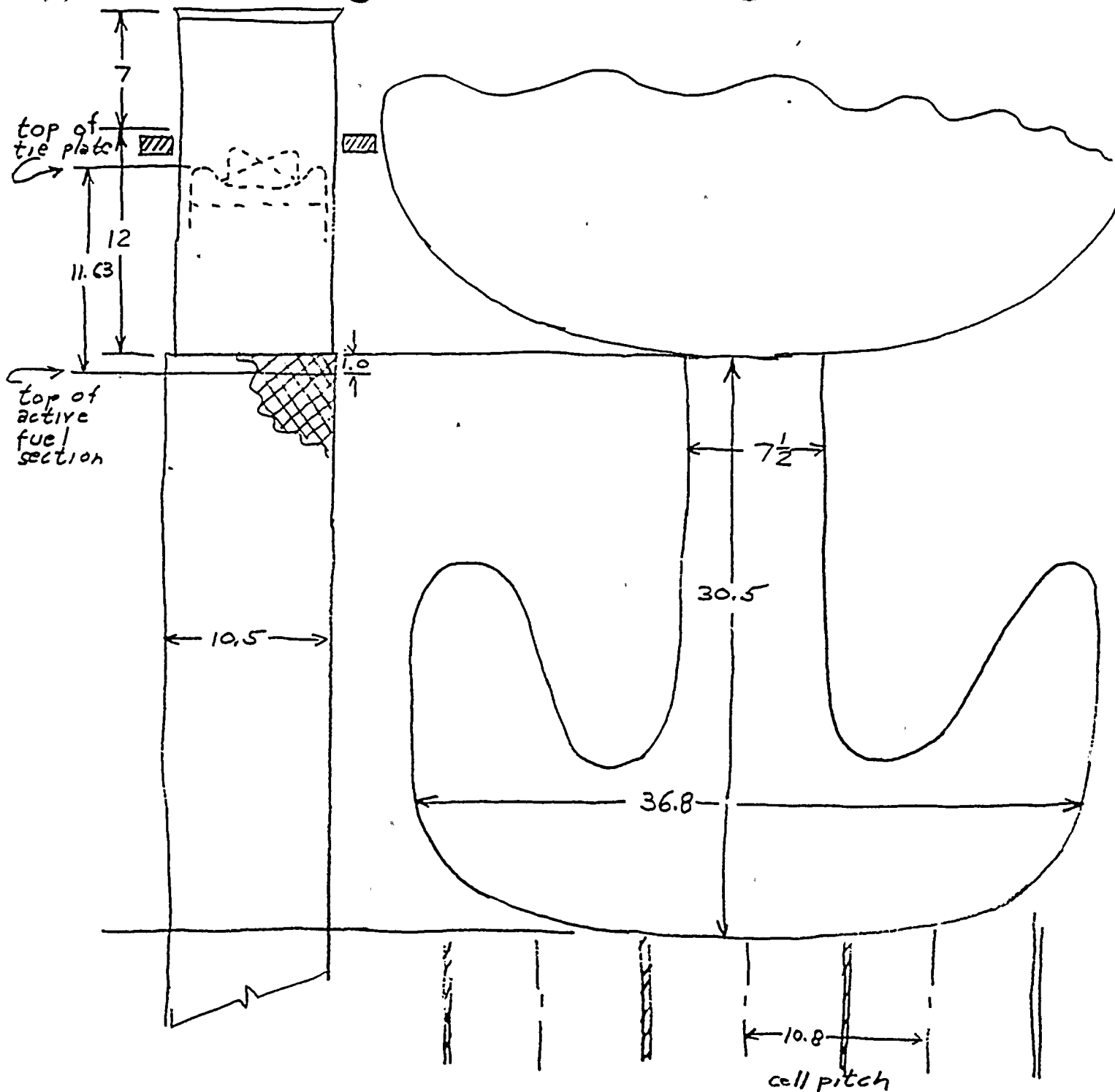
$$\text{True stress of bar \#2} \approx 42,000 + \frac{.0502}{1.36} (144,500 - 42,000) = 45,783 \text{ psi}$$

Energy absorbed by four bars \#2

$$= 4 \times 84.4 \left[\frac{42,000 + 45,783}{2} \right] .0502 = .743 \times 10^6 \text{ in}\#$$

$$\text{Total energy absorbed by 8 bars} = (1.63 + .743) \times 10^6 = \underline{2.37 \times 10^6 \text{ in}\#}$$

This is very close to the available energy of $2.16 \times 10^6 \text{ in}\#$. The slight difference is negligible



Extent of Penetration Into Fuel Rack

$$= 19 + 30.5 = 49.5 \text{ in}$$

$$\text{Penetration into Boral region} = 30.5 \text{ in}$$

$$\text{Penetration into fueled region} = 30.5 - 1.0 = 29.5 \text{ in}$$

Estimate the number of broken fuel rods and the number of fuel pellets which will be free to fall to the first undamaged spacer.

Referring to page A-9, assume that all of the rods are ruptured in four fuel assemblies

$$\text{No of ruptured rods} = 4 (264) = \underline{\underline{1,056}}$$

Assume that all of the active fuel displaced by the hook is released to the tank.

$$\text{Hook thickness} = 7.5 \text{ in}$$

$$\text{Rod pitch} = .496 \text{ in}$$

$$\text{Hook width} = 36.8 \text{ in}$$

No of rods damaged to the point where pellets are released

$$= \left(\frac{7.5}{.496} \times \frac{36.8}{.496} \right) \frac{\overset{\text{fueled rods}}{264}}{\underset{\text{total rods}}{289}} = 1024$$

$$\text{Linear length of fuel released} = 1024 \times 29.5 = 30,208 \text{ in}$$

$$\text{Wt released} = 143 \frac{\text{gU}}{\text{ft}} \times \frac{30,208 \text{ in}}{12 \frac{\text{in}}{\text{ft}}} \times \frac{1 \text{ Kg}}{1000 \text{ g}} = \underline{\underline{360 \text{ Kg U}}}$$

From Ref 5, the radiation released by the rupture of all fuel rods in one assembly is as given below. The release for 4 assemblies is simply 4 times as large

	thyroid	whole body
Release from 1 assembly (Ref 5)	1.8 rem	.53
" " 4 assemblies	7.2	2.12
10 CFR 100 limit/4	75	6.25

The 10 CFR 100 limits will not be exceeded

APPENDIX B

B-1

DETERMINATION OF AVERAGE CRUSHING FORCE

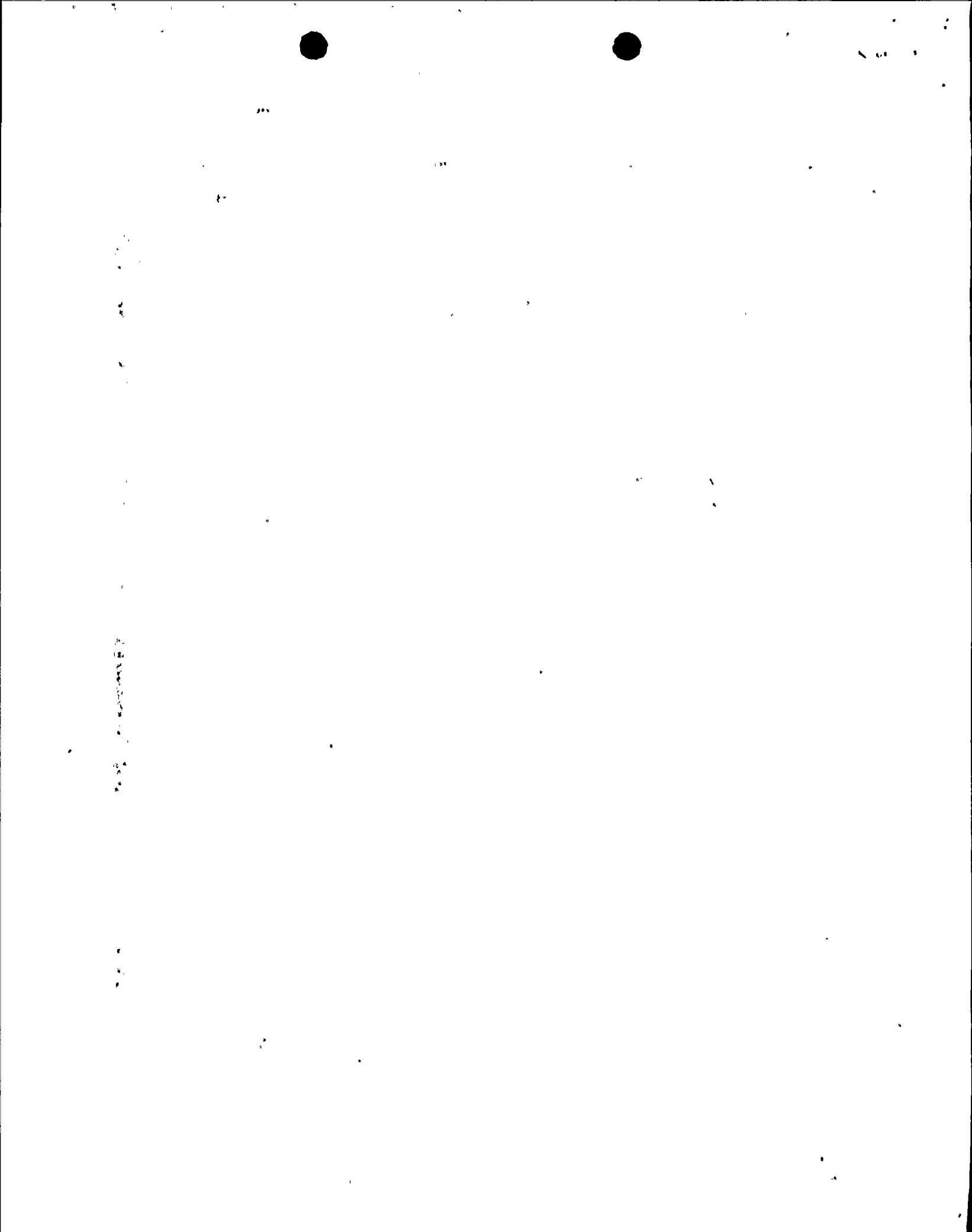
It is a simple matter to calculate the buckling load of the upper section of the fuel storage cell since it consists of a square duct. The duct is made up of four plates which are welded on the corners. When the buckling load is exceeded, two of the opposing plates will buckle inward while the other two plates buckle outward. In this way, the intersection of the plates remains a right angle, and no moment is transferred across the joint. This mode of deflection would absorb the least energy. Each of the four plates is then simply supported on all edges. Note on page A-8 (copied from Ref. 2) that the buckling load is independent of a/b for values of a/b greater than 0.8. This shows that the buckling of simply supported plates (and therefore thin walled ducts) is fundamentally different from that of thick walled columns. The thick walled column will collapse at the axial location of maximum bending moment, and thereafter form a plastic hinge. The applied load will fall off quickly, and therefore, very little energy will be absorbed. This happens because all of the energy is absorbed at the short plastic hinge. On the other hand, each of the sides of the thin walled duct will fail independently (at a relatively low load), but the corners provide sufficient restraint to avoid complete collapse. As explained in Reference 4 (page 38 attached), the plate elements continue to carry load after buckling. A periodic wave is formed in the thin walled column which means that many plastic hinges must occur in order to crush the column. It follows that the crushing of this thin walled column will absorb much more energy than the buckling of a thick walled column. This periodic deflection curve for the thin walled duct explains why the buckling load is nearly independent of the a/b ratio. The length of the column does not matter since each characteristic section of the column has its own buckling load.

In order to demonstrate this effect, two crushing tests were performed. The first was a 4.7 inch steel duct with a 25 mil wall. Page B-4 illustrates the geometry of the steel duct and shows the experimental data of load vs. deflection. A calculation of the critical stress and buckling load is also included. Notice that the measured load of 1.9 tons (or 3,800 lb.) is much higher than the calculated value of 1,430 lb. This is probably due to the fact that the duct was fabricated from two sheets of metal which were bent to shape and joined in two corners. The two joints consist of interlocking bends of metal and are, therefore, very stiff. Page B-5 shows the load-deflection curve. As the theory suggests, very high forces are maintained after buckling. The force dropped off to one-half of the initial buckling load, and occasionally dropped to values as low as one-fourth of the buckling load. It would be conservative to assume that the average crushing force is one-third of the buckling load.

In fact, the initial buckling load was exaggerated by the two stiffened joints. These joints probably contributed much more to the initial buckling strength than to the subsequent load carrying ability of the duct. The load carrying ability after buckling depends on the stretching and folding of the plates. If the two joints were not stiffened, the ratio of sustained crushing load to the initial buckling load would have been greater than 1/3.

Page B-6 shows two photographs of the partially crushed, steel duct. Note how two plates buckle outward, while the other two buckle inward. After this occurs, the load began to pickup again, and this will reoccur many times until the duct is completely crushed. One of the stiffened joints can be seen in the picture.

Page B-7 illustrates the geometry of the second buckling test. This was done with a soft aluminum extrusion with a thicker wall. The calculated buckling stress of 51,920 psi is much greater than the yield stress of this material which is probably less than 10,000 psi. The duct actually failed at a stress of 12,500 psi. Failure was initiated by yielding of the material rather than the application of the critical stress. The stress vs. deflection curve shown on Page B-8 shows an average crushing force of half the buckling force. The crushing pattern is much like the previous test. Note from the photographs on Page B-9 that this soft material experiences a great deal of deformation before the load picks up for the second collapse. As before, the duct will collapse many times until it is completely crushed. This test again confirms the fact that it is very conservative to assume that the average crushing load is equal to one-third of the buckling load.



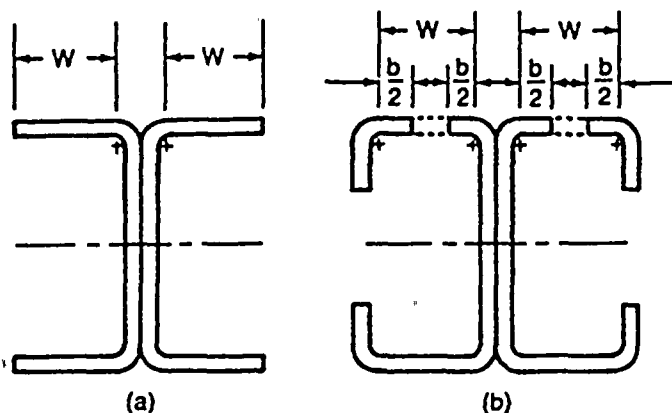


Fig. C.4 Flat Width and Effective Design Width of Flexural Members

Following the same approach used in Reference 4, the unit for stress has been changed to ksi in the 1974 Specification instead of psi used in the previous edition.

2.3 Properties of Sections

Unlike columns or shells, plate and sheet elements possess a large strength reserve after buckling, unless buckling occurs at stresses approaching the yield point for sharp yielding materials or at large inelastic strains for materials such as stainless steels which do not have a definite yield point. For example, Figure C.5(a) shows the buckled form of a stiffened compression element (a sheet which is supported along both unloaded edges by thin webs or edge stiffeners and can be regarded as simply supported), uniaxially loaded by a compression force. Although the element has buckled, and out of plane waves have developed, it is still capable of sustaining additional load, and the member of which the element is a part does not collapse. This behavior is a result of the mem-

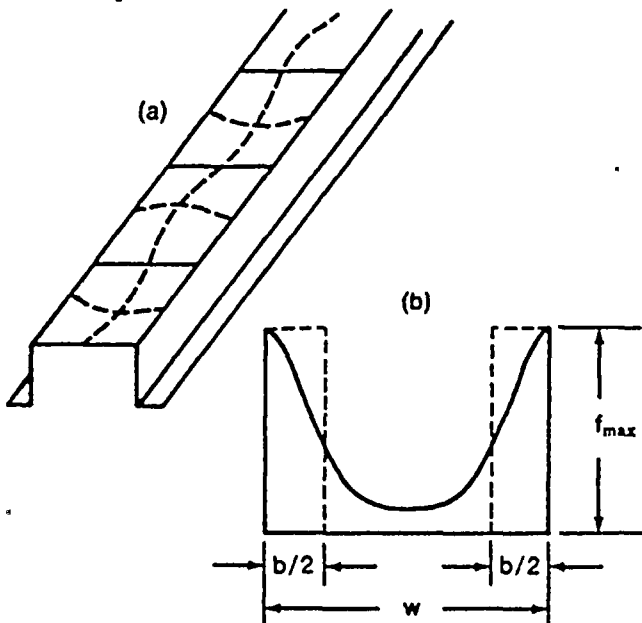


Fig. C.5 Local Buckling and Post Buckling Strength of Stiffened Compression Element

brane stresses which are developed in the element transverse to the direction of loading. Unstiffened elements (sheets which are supported along one unloaded edge only, the other unloaded edge being unsupported) behave in a similar fashion, except that the strength reserve after buckling is relatively small because less membrane action is possible.

The general equation for the critical buckling stress of isotropic sheet elements is

$$\sigma_{cr} = \frac{k\pi^2\eta E_o}{12(1-\mu^2)(w/t)^2} \quad (C.1)$$

where

- σ_{cr} = critical buckling stress
- E_o = initial modulus of elasticity
- μ = Poisson's ratio in the elastic range
- η = plasticity reduction factor
- w = flat width
- t = thickness
- k = buckling coefficient

Inspection of Eq. (C.1) reveals that the ratio of flat width to thickness of the sheet element is an important parameter; the critical stress decreases with increasing width-thickness ratio.

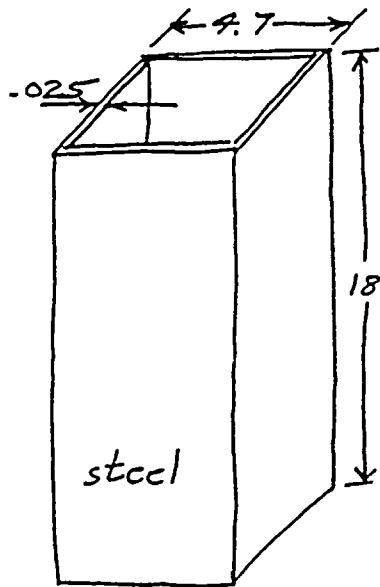
To keep the width-thickness ratio reasonably small, thus maintaining larger critical stresses, compression elements are frequently provided with intermediate longitudinal stiffeners between webs or between a web and an edge stiffener (Figure C.3).

In practical design the effective width concept is widely used for taking the postbuckling strength of compression elements into account. Figure C.5(b) indicates the post buckling stress distribution in a stiffened compression element. The solid line is the actual stress distribution over the actual element width, w . The dashed line is the equivalent uniform stress distribution, equal in intensity to the edge stress of the actual distribution but only applied over an effective width b . The total load carried by the element is the same for both distributions. Applications of the effective width concept are given in Section 2.3.1 of the Specification.

The effective width concept is used explicitly in computing the properties of sections which contain stiffened or multiple-stiffened compression elements. Because the effective width is a function of the element edge stress, it follows that the properties of the section are also functions of the stress level. For this reason, when computing the effective area, moment of inertia, and section modulus, proper recognition must be given to the effective width of stiffened and multiple-stiffened compression elements as a function of the edge stress and the flat-width ratio. The applications of the provision are included in Sections 2.4 and 3.6 of the Specification.

2.3.1.1 Stiffened Element Without Intermediate Stiffeners

The effective width relations used in the previous edition of stainless steel speci-



Load (tons)	Length (in)	Defl (in)
0	18	0
1.0	18	0
1.5		≈ .020
1.9	17 ^{15/16}	.063
1.2	17.9	.100
1.0	17 ^{7/8}	.125
1.1	17 ^{13/16}	.188
1.0	17.78	.220
1.0	17 ^{3/4}	.250
1.0	17 ^{11/16}	.313
.9	17 ^{5/8}	.375
.5	17 ^{9/16}	.438
.8	17.53	.470
.8	17.5	.500
.9	17.47	.530
.7	17 ^{3/8}	.625
1.0	17 ^{1/4}	.750
.9	17.0	1.00
.5	16 ^{7/8}	1.125
.7	16 ^{3/4}	1.25

$$\frac{d}{b} = \frac{18}{4.7} = 3.83$$

$$K = 3.29$$

$$E = 30 \times 10^6$$

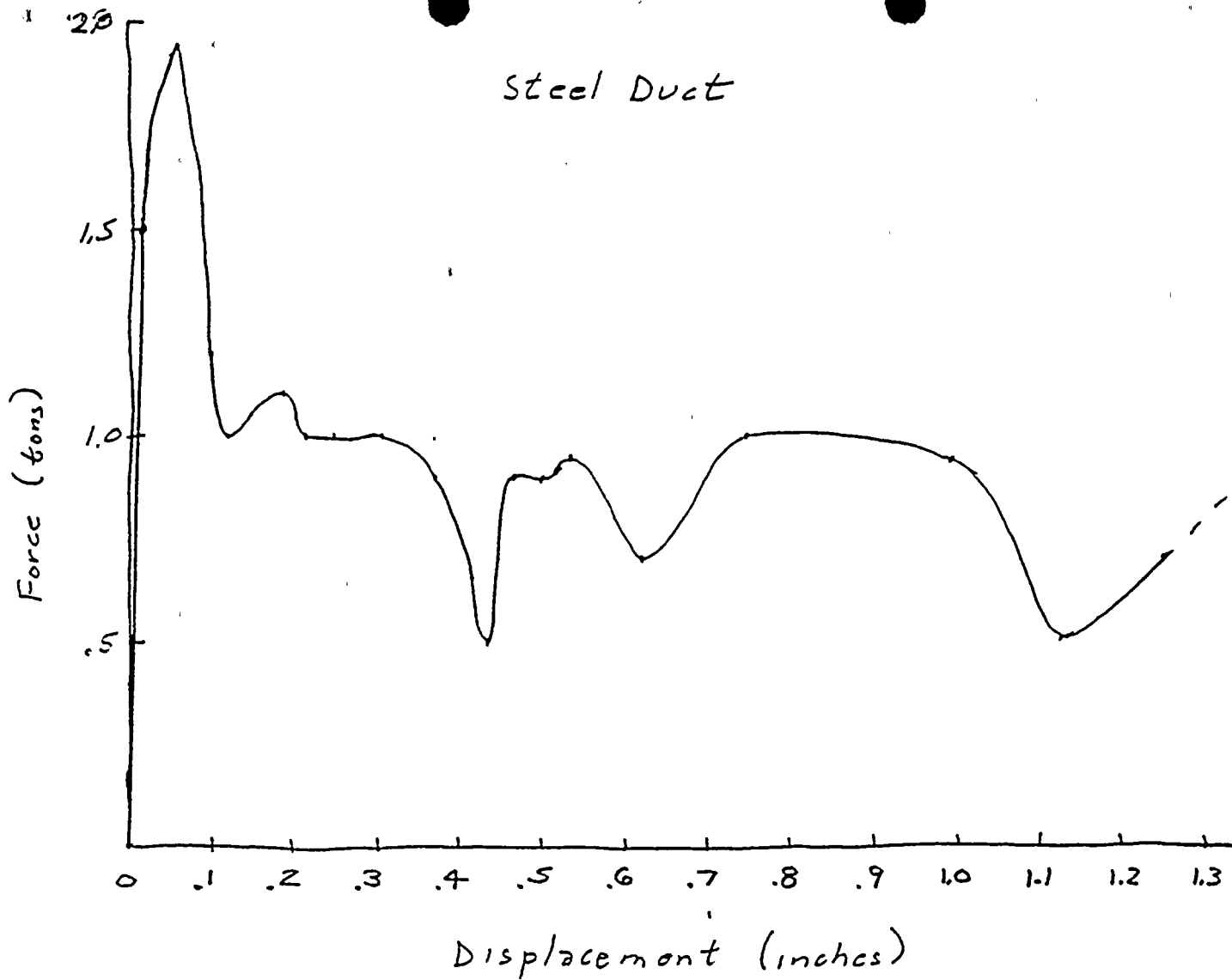
$$\nu = .287$$

$$S' = \frac{3.29 \times 30 \times 10^6}{1 - .287^2} \left(\frac{.025}{4.7} \right)^2 = 3,043 \text{ psi}$$

$$F = 3,043 (4.7 \times .025) 4 = 1,430 \text{ #}$$

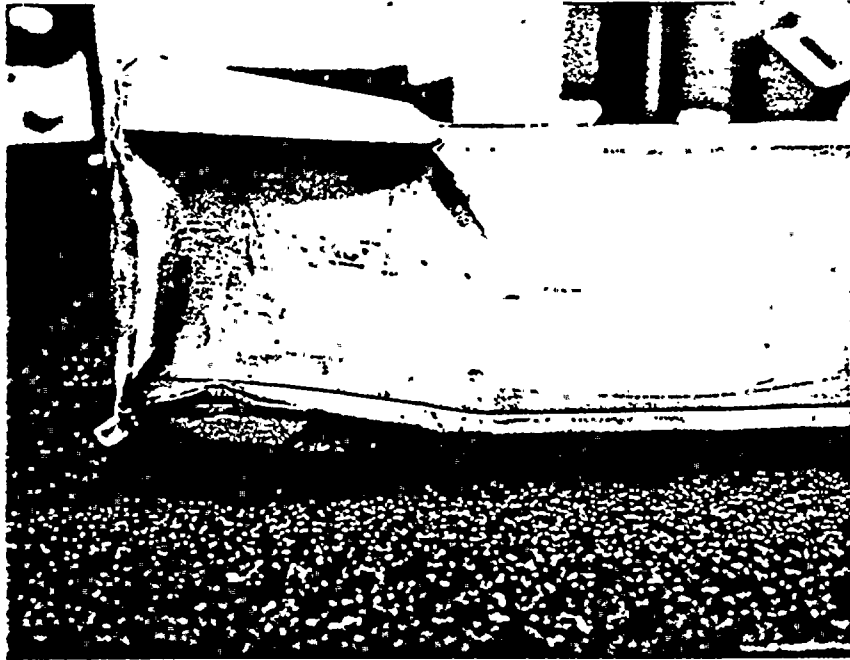
B-15

Steel Duct



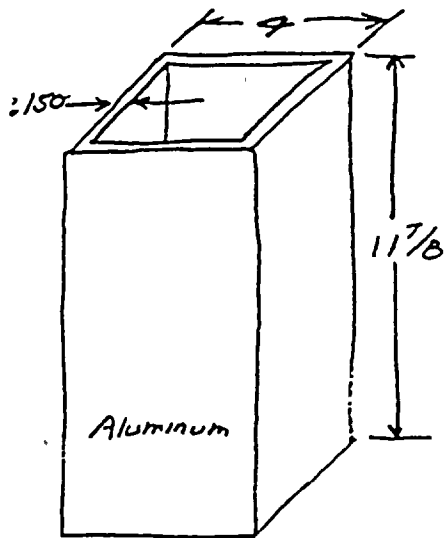
stress at 1.9 tons = $\frac{1.9 \times 2000}{4 \times 4.71 \times 0.025} = 8,085 \text{ psi}$

B-6



Steel Duct

B-7



Load (lbs)	Length (in)	Defl (in)
0	11.875	0
5	11.875	0
9	"	0
10	11.844	.031
11	11.844	"
12	"	"
13	"	"
14	11.813	.062
15	11.750	.125
12	11.688	.188
11	11.625	.250
9.5	11.563	.313
8	11.500	.375
7	11.438	.438
6	11.375	.500
5.5	11.313	.563
5.1	11.250	.625
5.1	11.188	.688
4.6	11.125	.750
4.1	11.000	.875
4.5	10.813	1.063
4.5	10.750	1.125
4.5	10.688	1.188
5.8	10.475	1.400
5.1	10.250	1.625
4.7	10.063	1.813
4.9	9.875	2.000
9.1	9.500	2.375
10.2	9.250	2.625
8.9	8.938	3.063

$$\text{Buckling Stress} = s' = \frac{\kappa E}{1-\nu^2} \left(\frac{t}{b} \right)^2$$

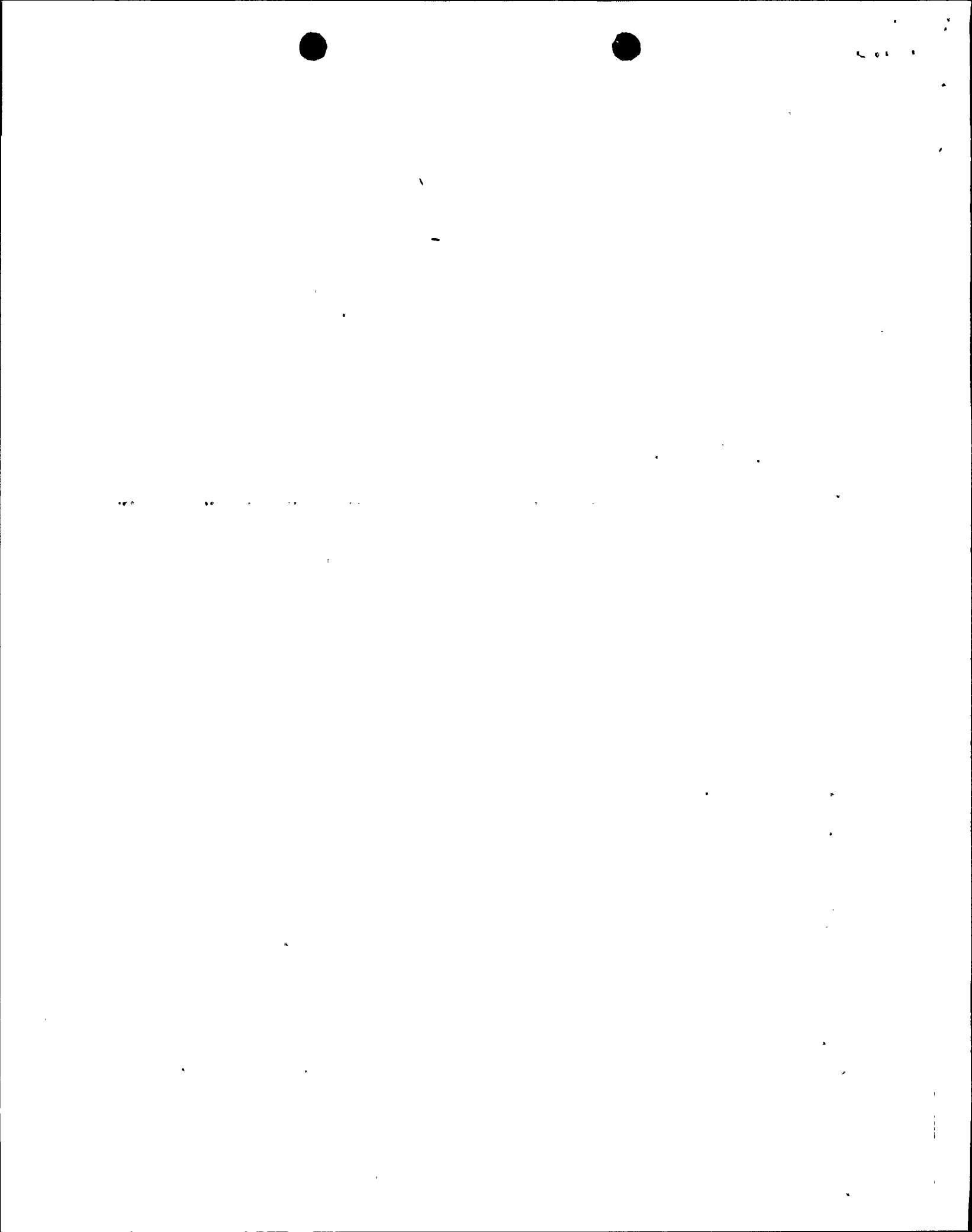
(all edges simply supported)

$$a/b = 11.875/4 = 2.97 \quad \kappa = 3.29$$

$$E = 10 \times 10^6 \quad \nu = .25$$

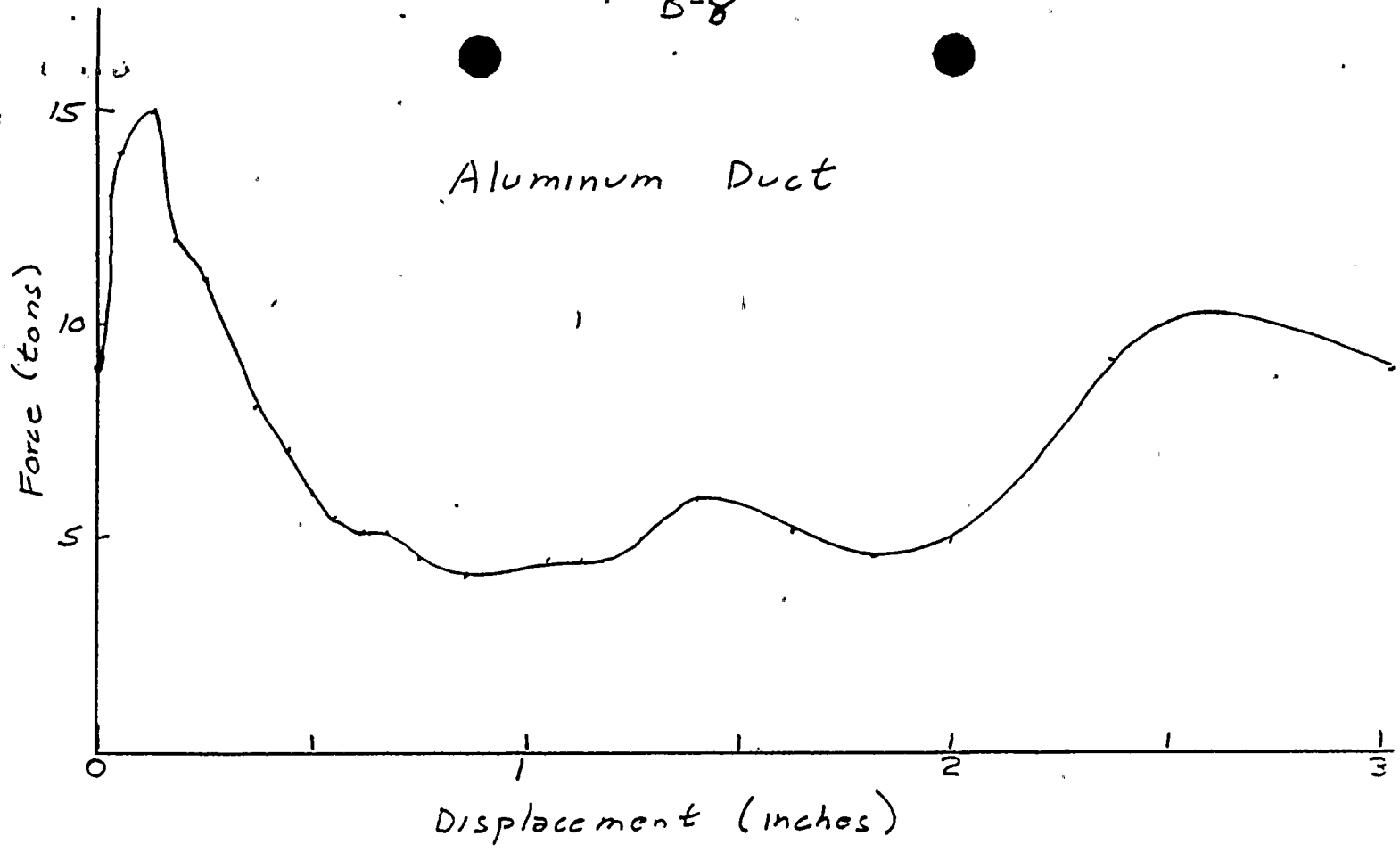
$$s' = \frac{3.29 \times 10^7}{1-.33^2} \left(\frac{.150}{4} \right)^2 = 51,920 \text{ psi}$$

$$\text{Stress at buckling load} = \frac{15 \times 2,000}{4 \times 4 \times .150} = 12,500 \text{ psi}$$



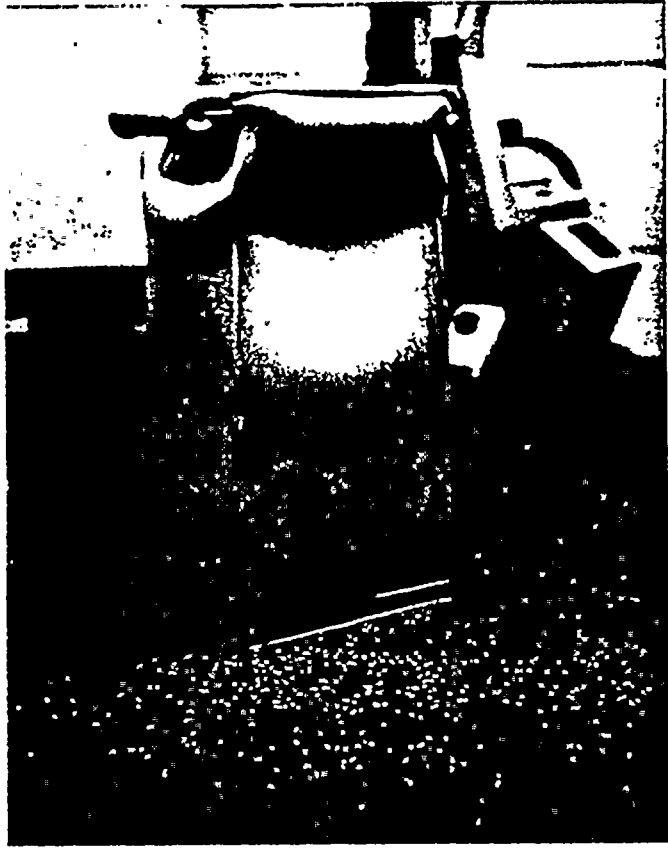
B-8

Aluminum Duct

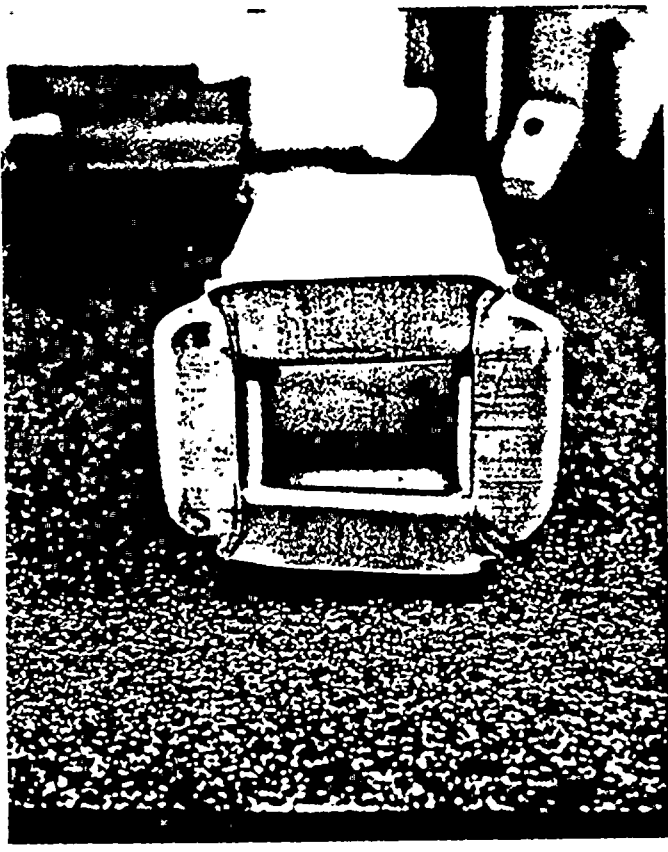


Stress at 15 tons = $\frac{15 \times 2000}{4 \times 4 \times .15} = 12,500 \text{ psi}$

B-9



Aluminum Duct



APPENDIX C

C-1

NITAWL INPUT LISTING

'DC COOK HOOK DROP, 4.0%ENR, EXPLICIT MODEL

0\$\$ 6 7 8 11 18 19 9 0 20

1\$\$ 0 21 5R0 10 2R0 -1 0

T

' FOR U-235,U-238: XXX0Y=UNDAMAGED, XXX2Y=DAMAGED

' Y=1 FOR INTERIOR RODS, Y=2 FOR EDGE RODS

' DAMAGED PITCH=0.52718", UNDAMAGED=0.496"

2\$\$ 92235 -92501 -92502 -92521 -92522

92238 -92801 -92802 -92821 -92822

40302 25055

8016 1001 24304 26304 28304 13027

5010 5011 6012

3** 92501 293.15 2 0.38481 0.2065 1773.7 9.40644-4 1
15.9994 185.225 1 238.051 196.683 1 192502 293.15 2 0.38481 0.1622 1773.7 9.40644-4 1
15.9994 185.225 1 238.051 196.683 1 192521 293.15 2.0 0.38481 0.1537 1773.7 9.40644-4 1.0
15.9994 185.23 1.0 238.051 196.68 1 192522 293.15 2.0 0.38481 0.1369 1773.7 9.40644-4 1.0
15.9994 185.23 1.0 238.051 196.68 1 192801 293.15 2 0.38481 0.2065 74.85 2.22902-2 1.0
15.9994 7.8165 1.0 235.044 0.4431 1.0 1.092802 293.15 2 0.38481 0.1622 74.85 2.22902-2 1.0
15.9994 7.8165 1.0 235.044 0.4431 1.0 1.092821 293.15 2.0 0.38481 0.1537 74.9 2.22902-2 1.0
15.9994 7.8165 1.0 235.044 0.4431 1.0 1.092822 293.15 2.0 0.38481 0.1369 74.9 2.22902-2 1.0
15.9994 7.8165 1.0 235.044 0.4431 1.0 1.040302 293.15 1.0 0.0635 0.2125 191.39 4.25181-2 1.0
6R0.0 1.0

' MN IN 304 SS, SLAB, AVG THK = 0.05", DANC=0.0

25055 293.15 1.0 0.127 0.0 511.83 1.73644-3 1.0

55.847 387.309 1.0 58.71 79.3401 1.0 1.0

4** F293.15

T

KENO-Va INPUT LISTING

DC COOK HOOK DROP, 4.0%ENR

READ PARAMETERS

TME=50.0 GEN=103 NPG=400 LIB=41 TBA=2.0

FLX=YES FDN=YES XS1=YES NUB=YES PWT=YES

END PARAMETERS

READ MIXT SCT=1

' INTERIOR ROD, UNDAMAGED BUNDLE

MIX=1 92501 9.4064-4 92801 2.2290-2 8016 4.6462-2

' EDGE ROD, UNDAMAGED BUNDLE

MIX=2 92502 9.4064-4 92802 2.2290-2 8016 4.6462-2

' INTERIOR ROD, DAMAGED BUNDLE

MIX=3 92521 9.4064-4 92821 2.2290-2 8016 4.6462-2

' EDGE ROD, DAMAGED BUNDLE

MIX=4 92522 9.4064-4 92822 2.2290-2 8016 4.6462-2

' ZIRCALLOY

MIX=5 40302 4.2518-2

' WATER

MIX=6 1001 6.6740-2 8016 3.3370-2

' 304SS FOR CAN

MIX=7 24304 1.7430-2 25055 1.7364-3 26304 5.9359-2 28304 7.7182-3

' ALUMINUM

MIX=8 13027 6.0242-2

MIX=9 5010 6.6707-3 5011 2.7081-2 6012 8.4380-3

END MIXT

READ GEOMETRY

UNIT 1

COM=' INTERIOR ROD, UNDAMAGED BUNDLE'

CYLI 1 1 0.38481 2P100.0

CYLI 0 1 0.3937 2P100.0

CYLI 5 1 0.4572 2P100.0

CUBO 6 1 4P0.62992 2P100.0

UNIT 2

COM=' EDGE ROD, UNDAMAGED BUNDLE'

CYLI 2 1 0.38481 2P100.0

CYLI 0 1 0.3937 2P100.0

CYLI 5 1 0.4572 2P100.0

CUBO 6 1 4P0.62992 2P100.0

UNIT 3

COM=' GUIDE TUBE, UNDAMAGED BUNDLE'

CYLI 6 1 0.3937 2P100.0

CYLI 5 1 0.4572 2P100.0

CUBO 6 1 4P0.62992 2P100.0

UNIT 4

COM=' INTERIOR ROD, DAMAGED BUNDLE'

CYLI 3 1 0.38481 2P100.0

CYLI 0 1 0.3937 2P100.0

CYLI 5 1 0.4572 2P100.0

CUBO 6 1 4P0.669514 2P100.0

UNIT 5

COM=' EDGE ROD, DAMAGED BUNDLE'

```

CYLI 4 1 0.38481 2P100.0
CYLI 0 1 0.3937 2P100.0
CYLI 5 1 0.4572 2P100.0
CUBO 6 1 4P0.669514 2P100.0
UNIT 6
COM=' GUIDE TUBE, DAMAGED BUNDLE'
CYLI 6 1 0.3937 2P100.0
CYLI 5 1 0.4572 2P100.0
CUBO 6 1 4P0.669514 2P100.0
UNIT 7
COM=' UNIT 7 IS UNDAMAGED BUNDLE'
ARRAY 1 2*-10.70864 -100.0
REPLICATE 6 1 4R0.6731 2R0.0 1
REPLICATE 7 1 4R0.1905 2R0.0 1
REPLICATE 8 1 4R0.0254 2R0.0 1
REPLICATE 9 1 4R0.18034 2R0.0 1
REPLICATE 8 1 4R0.0254 2R0.0 1
REPLICATE 7 1 4R0.0762 2R0.0 1
REPLICATE 6 1 4R1.45542 2R0.0 1
UNIT 8
COM=' UNIT 8 IS DAMAGED BUNDLE, PITCH=0.5272"'
ARRAY 2 2*-11.38174 -100.0
REPLICATE 7 1 4R0.1905 2R0.0 1
REPLICATE 8 1 4R0.0254 2R0.0 1
REPLICATE 9 1 4R0.18034 2R0.0 1
REPLICATE 8 1 4R0.0254 2R0.0 1
REPLICATE 7 1 4R0.0762 2R0.0 1
REPLICATE 6 1 4R1.45542 2R0.0 1
ARRAY 3 3*0.0
COM=' ARRAY 3 IS 10X10 BUNDLE ARRAY'
END GEOMETRY
READ ARRAY
ARA=1 NUX=17 NUY=17 NUZ=1
LOOP
2 1 17 1 1 17 1 1 1 1
1 2 16 1 2 16 1 1 1 1
3 6 12 3 3 15 12 1 1 1
3 4 14 10 4 14 10 1 1 1
3 3 15 3 6 12 3 1 1 1
END LOOP
ARA=2 NUX=17 NUY=17 NUZ=1
LOOP
5 1 17 1 1 17 1 1 1 1
4 2 16 1 2 16 1 1 1 1
6 6 12 3 3 15 12 1 1 1
6 4 14 10 4 14 10 1 1 1
6 3 15 3 6 12 3 1 1 1
END LOOP
ARA=3 GBL=3 NUX=10 NUY=10 NUZ=1
LOOP
7 1 10 1 1 10 1 1 1 1

```

8 5 6 1 5 6 1 1 1 1
END LOOP
END ARRAY
READ START
NST=5 NBX=8
END START
READ BOUNDS
ALL=SPECULAR
END BOUNDS
END DATA

ATTACHMENT 2 TO AEP:NRC:0514R

**STEVENSON & ASSOCIATES**

a structural-mechanical consulting engineering firm

9217 Midwest Avenue • Cleveland, Ohio 44125 • (216) 587-3805 • Telex: 980101

1608C
86C1438

January 5, 1987

Rbb *1/6/87*
Mr. R. B. Bennett
American Electric Power Service Corporation
1 Riverside Plaza
P.O. Box 16631
Columbus, OH 4321-6631

Dear Mr. Bennett:

Per your and Mr. Satyan Sharma's request, I have performed an independent review of the mechanical analysis of the D.C. Cook Spent Fuel Pit Load Drop Analysis transmitted to you by letter from A.J. Martenson of the Exxon Nuclear Company Inc. dated 7 November 1986 and revision 2 of Appendix A and a new Appendix B to that Analysis transmitted to you on or about 31 December 1986. Based on this review, it is my opinion that the depth of penetration of a free fall drop of the crane book assembly into the spent fuel pool and impacting the spent fuel racks of 19 inches for the block plus 30.5 inches more for the hook is a reasonable estimate of the expected depth of penetration. Please advise if you require any clarification of this letter.

Sincerely,

John D. Stevenson
John D. Stevenson
President

cc: Mr. Satayan Sharma